J Seismol (2020) 24:803–832
https://doi.org/10.1007/s10950-020-09904-9

ORIGINAL ARTICLE

An updated parametric catalog of historical earthquakes around the Dead Sea Transform Fault Zone

Iason Grigoratos · Valerio Poggi · Laurentiu Danciu · Graciela Rojo

Received: 8 April 2019 / Accepted: 8 January 2020 / Published online: 14 February 2020

Abstract In this study, we present the work done to review the existing historical earthquake information of the Dead Sea Transform Fault Zone (DSTFZ). Several studies from various sources have been collected and reassessed, with the ultimate goal of creating of new homogenized parametric earthquake catalog for the region. We analyze 244 earthquakes between 31 BC and 1900, which are associated with the geographical buffer extending from 27 N to 36 N and from 31 E to 39 E. Of these, 93 were considered real seismic events with moment magnitude (M_w) greater than 5 that indeed occurred within this zone. While we relied on past parametric data and did not assign new macroseismic intensities, magnitude values, or epicenters for several controversial events, we did however resort to the primary sources to obtain a more critical perspective for the various assigned macroseismic intensities. In order to validate the derived parametric information, we tried to associate the events present in the historical records, with any evidence coming from past field investigations, i.e., geological or archaeological studies. Acknowledging the uneven quality and quantity of data reporting each event, we provided each entry with an uncertainty range estimate. Our catalog lists 33 events of $M_w \geq 6$ absent from the latest published compilation with compatible time span and areal coverage. The whole catalog is considered complete down to M_w 7 and in certain areas down to M_w 6 after the year 1000, with majority of the larger earthquakes located in the part of DSTFZ, which extends from the southeast part of Dead Sea lake till Antioch.

Keywords Parametric catalog · Middle East · Paleoseismic · Seismites · Faults · Magnitude

Article Highlights
- We reviewed 244 earthquakes mentioned in historical records, geological investigations, and archaeological studies.
- We list parametric information for 93 earthquakes with magnitude greater than 5 that occurred between 31 BC and 1900.
- Our catalog lists several earthquakes with magnitude greater than 6 that are absent from previous compilations.

Electronic supplementary material The online version of this article (https://doi.org/10.1007/s10950-020-09904-9) contains supplementary material, which is available to authorized users.

I. Grigoratos (✉)
University School of Advanced Studies IUSS Pavia, Pavia, Italy
e-mail: iason.grigoratos@iusspavia.it

V. Poggi
National Institute of Oceanography and Applied Geophysics (OGS), Udine, Italy

L. Danciu · G. Rojo
ETH Zurich, Zurich, Switzerland

1 Introduction

Seismic hazard assessment is often performed in a probabilistic way, based on the observed recurrence rates of earthquakes (e.g., Woessner et al. 2015). The latter can be measured or inferred in many ways (Field et al. 2014), but the most common approach is the analysis of observed seismological data, e.g., from instrumental recordings. Unfortunately, direct observations are available for a relatively short time span when compared with

the average return period of large magnitude earthquakes. The latter are indeed rare, since they are the product of a slow geological process of strain accumulation, and thus require a long observation period to be properly characterized in a statistical sense. Integration with non-direct evidence of past historical seismicity is therefore essential to properly constrain low probabilities of occurrence in seismic hazard assessment.

Pre-instrumental sources of information comprise any documented descriptions of an earthquake and its effect on the society (e.g., damage to buildings) or on the environment (e.g., modification of the landscape) (Albini et al. 2014). Written historical data can thus be very useful, even though they can be subjective and ambiguous. Relevant primary sources are often scattered and obscure, in a variety of languages and scripts, and frequently reflect the cognitive bias of contemporary writers to associate natural disasters with theological and political morals (Karcz 2004; Ambraseys 2005b). The identification of historical events is thus a rather multi-disciplinary procedure, which combines historical and cultural knowledge, engineering judgment, seismological background, and interpretation of geological and archeological evidence. Comparing independent and heterogeneous sources of information enables one to evaluate the uncertainty surrounding each seismic event, while combining them adds important constraints to the definition of more objective parametric results. The present study treats this complex task with a certain methodology, aiming at presenting an updated historical earthquake catalog for the Dead Sea Transform Fault Zone (DSTFZ), tailored for use in seismic hazard assessment.

The demand for seismic hazard estimates is particularly high in the region around the DSTFZ, where several seismic risk mitigation efforts are taking place (Grigoratos et al. 2016; Kottmeier et al. 2016; Grigoratos et al. 2018a). Although the DSTFZ has produced several destructive events in the past, many places around it are characterized by a large percentage of non-seismically designed buildings, hence being particularly vulnerable to earthquakes. In some countries, the population is not fully aware of the seismic risk, due to the (temporary) quiescence of the fault zone in recent years. As a matter of fact, only two earthquakes with $M_w \geq 6$ have occurred along the DSTFZ in the last century (Ambraseys 2006). Long-term observations over the past 2100 years along the DSTFZ however are very different. There have been many earthquakes that destroyed entire cities, caused great loss of life, and affected the economic growth of certain centers (e.g., in 31 BC, 115, 551, 1033, 1170, 1202, 1759) (Ambraseys 2009).

Although many descriptive historical catalogs do exist for the region (§4.1), only two of the available parametric ones span a wide enough geographical coverage and time period. The first catalog, EMEC (Gruenthal and Wahlstroem 2012), was used in the SHARE project (Woessner et al. 2015), while the second one, by Zare et al. (2014), was compiled for the EMME project (Danciu et al. 2017). Within our region of interest (27 N–36 N and 31 E–39 E), EMEC does not consider events before the year 300, while the catalog by Zare et al. (2014) does not list around 30 damaging events listed in multiple descriptive sources. Both parametric catalogs are mainly based on historical sources, with limited cross-examination of the available field data (§4.2). Additionally, some of their conclusions are challenged by newly published studies. For these reasons, we decided to reappraise the reported historical earthquakes and their correlated field evidence and compile an updated parametric historical earthquake catalog for the DSTFZ. Combined with the updated instrumental catalog for the region (Grigoratos et al. 2020), our study offers nearly 2050 years of homogenized historical earthquake data, tailored for use in seismic hazard assessment studies (e.g., Grigoratos et al. 2018b).

2 Seismotectonic setting

The Dead Sea Transform Fault Zone (DSTFZ) consists of a sequence of left-lateral transform faults connecting the spreading ridge of the Red Sea in the south with the compressional deformation zones of the Arabia-Eurasia collision zone in the north (Garfunkel et al. 1981). It includes several pull-apart basins (Fig. 1), lakes, and push-up zones. The DSTFZ is mostly confined to a relatively narrow zone, less than 100 km wide, but spreads out close to the Lebanon restraining bend and the Palmyrides in the North (Ambraseys 2009). The fault system is highly segmented; hence, ruptures are likely limited in length due to structural discontinuities or bends. Seismicity is rather diffuse along the system, with epicenters localized both within and nearby the main lineaments. Although the large majority of earthquakes are localized at depths between 10 and 20 km,

the total seismogenic thickness beneath the Dead Sea lake is about 28 km (Aldersons & Ben-Avraham 2014).

In recent times, there is an apparent quiescence of the DSTFZ. Excluding the large earthquake of November 22, 1995 (surface magnitude M_s 7.1) in the Gulf of Aqaba, only one mainshock of M_s 6.0 or larger has occurred during the past century, in July 11, 1927 (Ambraseys 2001). The seismic activity of the last 2000–3000 years, however, is quite different, as demonstrated in the following. Global positioning system (GPS) measurements indicate significant crustal motion with slip rates of about 4–5 mm year^{-1} for the whole DSTFZ, perhaps somewhat larger north of Dead Sea lake and smaller further south (Marco & Klinger 2014; Am09). Garfunkel (2009) notes that approximately 1–2 Myr ago, the slip rate slowed to 4.0–5.5 mm year^{-1}, compared with an average rate of 6–7 mm year^{-1} over the past 5 Myr.

3 Methodology

For the creation of a homogenized historical parametric earthquake catalog for the DSTFZ, we first collected and reviewed available descriptive information from peer-reviewed articles and books, to create a preliminary list of significant earthquakes. Then, we compared this list with existing parametric historical catalogs (§4.1). We relied on past parametric data and did not assign new macroseismic intensities, magnitude values, or epicenters. For several controversial events, we did however resort to the translated original sources (herein also called contemporary or primary sources) in order to obtain a more critical perspective for the various assigned macroseismic intensities. In order to validate the derived parametric information, we tried to associate the events present in the historical records, with any evidence coming from past field investigations, i.e., geological or archaeological studies (§4.2).

The case study region has been the subject of several past studies (§4.1) due to its historical importance and tectonic domain. As a result, for most large historical events, several estimates of origin time, magnitude, and location are available in the literature. To address this issue, we had to evaluate and prioritize the parametric sources accounting also for their agreement with the field investigations (§5.2). Although a general hierarchy was defined based on qualitative considerations, in the end, each event was evaluated separately (Fig. 2). We paid special attention to properly annotating all the original sources (Appendix D) in order to render the procedure as transparent and reproducible as possible.

The resulting catalog was homogenized in moment magnitude (M_w) (Table 4), flagged for fore/aftershocks, and assessed in terms of uncertainty (§5.3) and completeness (§6.2).

A literature review on "piecewise" methodologies similar to the flowchart presented in Fig. 2 yielded limited results. To the best of our knowledge, only four past studies have relied solely on older sources of parametric information to compile a fully parameterized historical catalog of earthquakes. These four compilations are Khair et al. (2000), Gruenthal and Wahlstroem (2012; EMEC), Albini et al. (2014; GEM), and Zare et al. (2014; EMME). Khair et al. (2000) relied heavily on the solutions of Ben-Menahem and prioritized the parametric values that are closer to the mean of the observed range, without a critical evaluation of the damage distribution. The articles by Gruenthal and Wahlstroem (2012) and Zare et al. (2014) focus mainly on the instrumental part of the catalogs and do not clarify the rationale behind the parameterization of the historical events. Albini et al. (2014) followed a methodology that is similar to our approach; they treated most events on "an earthquake-by-earthquake basis" and selected as primary source the study in which the epicenters are most consistent with the available historical information. Regarding the magnitude, they prioritized values that were available in M_w or M_s. Contrary to our approach, they did not assign their own uncertainty classes, and rather listed uncertainty estimates only when such values were part of the original regression. Even though the selection of location and magnitude solutions is often subjective, a rigorous assessment on whether an event is reliably reported was proposed by Zohar et al. (2016; 2017). They came up with a four-step scheme that checks the number of primary and secondary sources to assign each event to five confidence levels, one of which considers the event spurious.

4 Review of sources

4.1 Historical data

In the historical times, the DSTFZ was politically unstable, mostly under the rule of successive invaders and

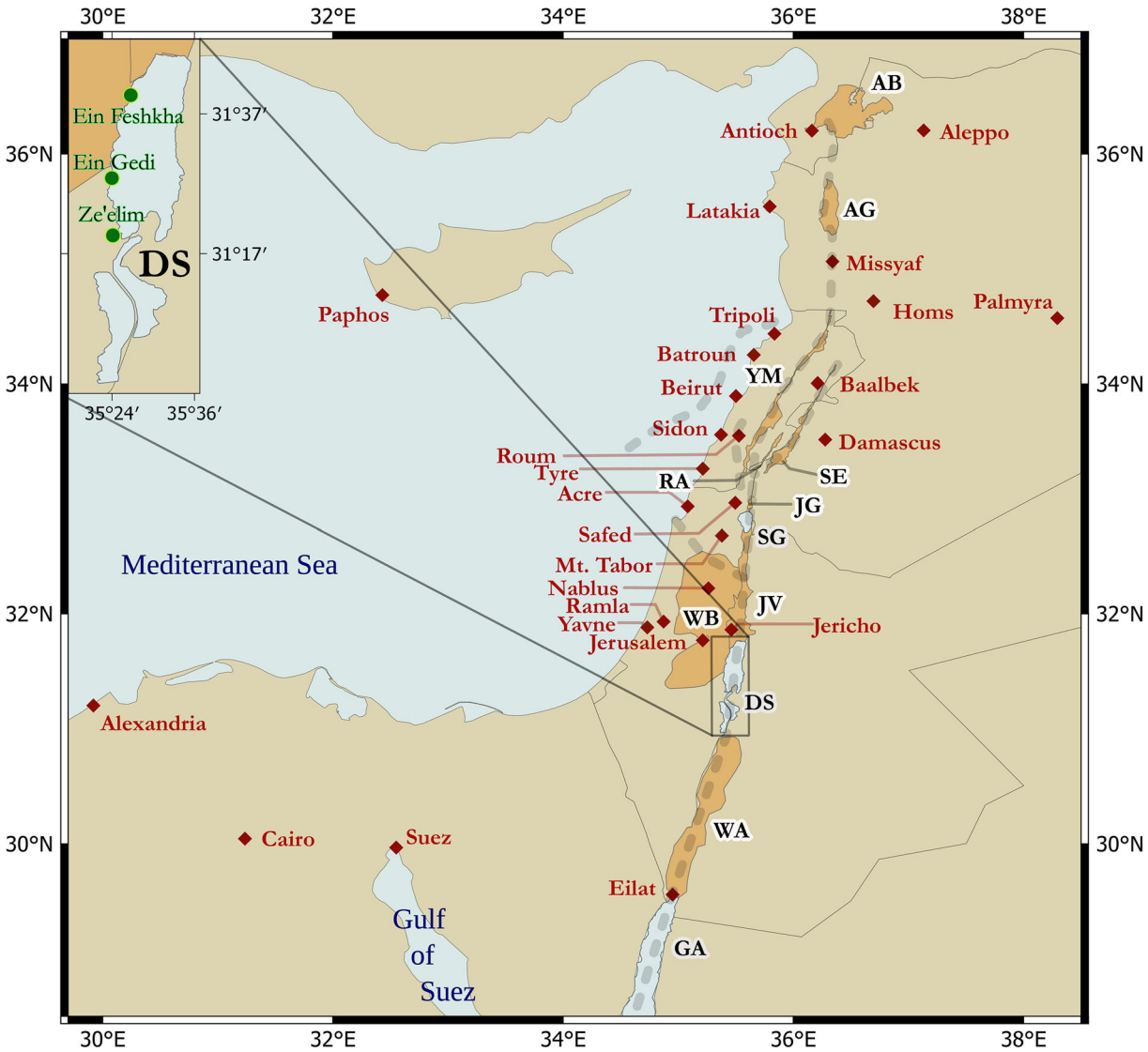

Fig. 1 Map of the Middle East showing the most relevant toponyms to the present study. AB, Amik Basin; AG, AlGhab Basin; DS, Dead Sea; GA, Gulf of Aqaba; JG, Jordan Gorge; JV, Jordan Valley; RA, Rachaya; SG, Sea of Galilee (aka Lake Kinneret or Tiberias); SE, Serghaya; WA, Wadi Araba; WB, West Bank; YM, Yammouneh. The orange color indicates important basins, while the dashed gray lines represent the major faults of the DSTFZ

oppressors (Karcz 2004). Consequently, the main references of seismic events are in chronicles and texts written in various languages, at distant administrative centers of the day. It should be noted that some authors of these texts sometimes subjectively explained the earthquakes as theological signs, whereas devastating effects on a distant or isolated province may have been overshadowed by lesser effects in more important parts of the regime (Karcz 2004; Ambraseys 2005b).

Nevertheless, the region is one of the few areas worldwide where historical accounts of earthquakes can date back many years BC. A careful and critical interpretation of these raw historical data is mandatory in order to build or evaluate descriptive catalogs of events, which are subsequently the basis of any parametric catalog for seismic hazard assessment. This process has been tackled by several past studies, whose quality and reliability however varies. The key descriptive and parametric earthquake catalogs for the region

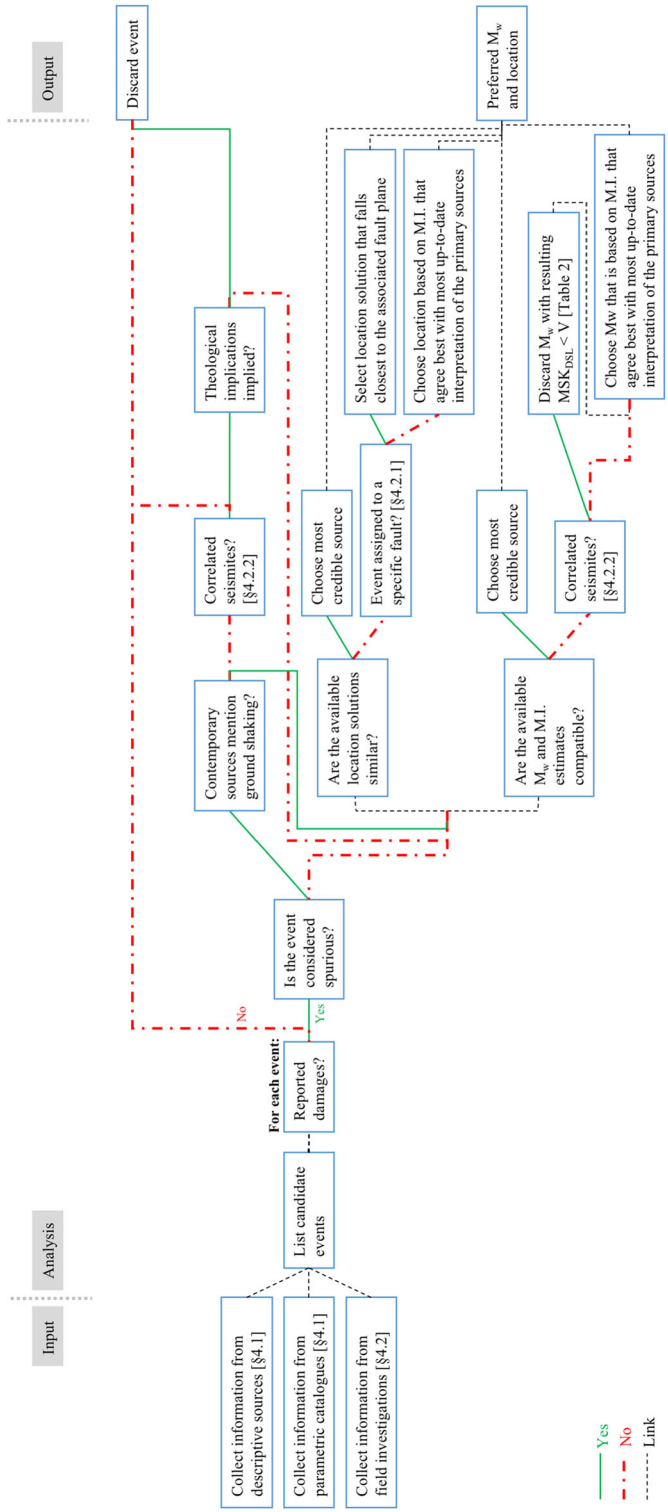

Fig. 2 Descriptive representation of the framework proposed to reappraise historical earthquakes and field investigation studies. All lines are directed from the right edge of each rectangle to the left edge of the next. M_w, moment magnitude; M.I., macroseismic intensities

that we examined are listed below in chronological order. A list of past bibliographic studies on specific historical events can be found in Appendix C1.

- Willis (1928) compiled an earthquake catalog for Palestine, between 1606 BC and 1927. As pointed out by Ambraseys (1962), it contains several errors and its contents should be treated carefully.
- Sieberg's annotated world catalog of earthquakes (1932) (Sieb32) includes isoseismal maps for the largest historical earthquakes worldwide up to 1930. His work, as he himself admits, is subjective. His catalog contains known errors and duplications in entries and gives little indication of his sources of information (Ambraseys 2009; Albini et al. 2018). His valuable work should be treated with caution.
- Amiran (1950; 1952) presented in 1950 and 1952 a revised catalog of Willis' work. In total, it contains around 180 events and sometimes provides Mercalli-Cancani-Sieberg (MCS) intensities. He updated the catalog 44 years later (Amiran et al. 1994) (Ami94) using Universal Time (UT) and the Modified Mercalli Intensity (MMI) scale (Wood & Neumann 1931), namely, the English translation of MCS.
- The catalogs of earthquakes in the Middle East by Ben-Menahem (1979) (BM79) (1991) (BM91) contain information extracted from earlier catalogs of varying quality (mainly Sieberg's) and from secondary works. These lists, which include a parametric catalog going back to 2050 BC, should be used with great caution. They are one of the earliest sources of magnitude values (local magnitude scale M_L), which are sometimes accompanied by MMI estimates. The source of the events and the rationale behind the estimated magnitude are often not given.
- The catalog of Poirier and Taher (1980) (PoTa80) covers the seismicity of the Middle East, listing nearly 200 events up to 1800. Even though the catalog contains some errors and duplications, it summarizes information taken from a thorough survey of Arabic material. The primary sources are properly cited. It also provides approximate coordinates of the affected cities and MMI estimations.
- The descriptive book by Ambraseys et al. (1994) (Am94) presents a thorough re-evaluation of seismicity in Egypt, Saudi Arabia, and the Red Sea. It is based on primary Persian, Arabic, and occidental sources, which are cited. It includes a parametric catalog with many approximate epicentral coordinates and Medvedev-Sponheuer-Karnik (MSK) intensities for events between 184 BC and 1899. It also contains few magnitude estimates and maps.
- The 1994 book by Guidoboni et al. (1994) (INGV94) describes earthquakes in the Mediterranean area up to the tenth century. Events are annotated and the primary sources are translated and properly cited. The book also provides a parametric catalog with the affected sites and maximum observed intensities, in both MCS and EMS scale (Gruenthal 1998). This catalog has been later converted into an online geo-referenced fully parametric catalog (Guidoboni et al. 2019) (INGVweb, http://storing.ingv.it/cfti/cfti5/#). The latter, in contrast to the book, also provides magnitude estimations and epicentral coordinates.
- Sbeinati et al. (2005) (Sb05) studied the historical earthquakes in Syria. Their sources are properly cited. They presented a list of 181 events (affected cities and EMS-92 intensities), together with a parametric catalog for 36 of them. For the latter, they estimated epicentral coordinates and surface wave magnitudes (M_s). They used isoseismal maps and the nomograph by Shebalin (1970). Their work has been proven valuable to this study.
- The 2005 book by Guidoboni and Comastri (2005) (INGV05) consists of a compilation of information about earthquakes in the Mediterranean region and in the Middle East over the period 1000–1500. This impressive catalog is written in similar style with the 1994 book by Guidoboni et al. and lists 383 events, of which 154 belong to Italy. The authors have used the "Boxer" method (Gasperini et al. 1999; Gasperini 2004) to calculate the epicentral coordinates and the equivalent moment magnitude (M_e), from geo-referenced MCS-assigned macroseismic intensities. As with INGV94, this catalog has been also merged into an online geo-referenced catalog (Guidoboni et al. 2019). The latter often provides magnitude estimations even when the 2005 book, due to limited intensity data, does not. Both the books and the geo-referenced catalog were a valuable source of descriptive and parametric information for this study.
- The book of Ambraseys (2009) (Am09) consists of a comprehensive descriptive catalog for the Mediterranean and Middle East until the year 1900. Primary sources are properly identified, cited, and when

necessary quoted. Entries that concern Egypt and the Red Sea are mostly identical to Am94. However, unlike the former, the 2009 book does not provide a parametric catalog with epicentral coordinates and intensities. Nevertheless, it contains critical descriptive information regarding the dating of events, affected areas, and tries to identify potential amalgamation of events or duplications. It also contains some isoseismal maps derived from previous studies of the author. The 2009 book occasionally compares its findings with what previous catalogs have reported (e.g., INGV94 or INGV05). This book, and the work of Ambraseys in general, was a key reference point throughout the course of this study.

- The European-Mediterranean Earthquake Catalog (EMEC) (Gruenthal and Wahlstroem 2012) contains events with $M_w \geq 6$ since year 300 and $M_w \geq 4$ since year 1000 in Europe and the Mediterranean area. The parametric information has been derived from previous studies, e.g., INGV94, INGV05, Sb05, and Feldman and Amrat (2007). EMEC often converts Khair et al.'s (2000) M_s values to moment magnitude. These M_s values however are already converted from original M_L estimates of Ben-Menahem. This sequential conversion may have led to increased uncertainty in the final homogenized values.
- The Global Earthquake Model (GEM) published a global parametric catalog of earthquakes between 1000 and 1903, which they considered complete for earthquakes above M 7 (Albini et al. 2014). They followed a transparent and refined methodology. The catalog contains 16 events within our investigated area, whose assigned epicentral coordinates and M_s values are derived from papers of Ambraseys or from Sb05. There is also an informative online geo-referenced version of this archive (https://emidius.eu/GEH/map.php).
- Within the framework of the large-scale "Earthquake Model of the Middle East Region" (EMME) project (Danciu et al. 2016; Danciu et al. 2017), Zare et al. (2014) compiled a parametric historical catalog since 31 BC for the Middle East. It contains 44 events within our investigated zone and provides epicentral coordinates and moment magnitude values, derived mostly from previous studies. For a few events, the source of the parametric values remains unclear.

4.2 Utilization of field investigations in parametric earthquake catalogs

The DSTFZ not only has long historical records but also stands out in the richness of archaeological and geological earthquake-related evidence, including tsunami reports (Salamon et al. 2007). That enables cross-evaluation of these three individual datasets. The mutual independency of these sources is not always warranted, and circular reasoning should be avoided carefully (Karcz 2004; Ambraseys 2005b; Rucker & Niemi 2010). We should clarify that even though the evidence from geology and archaeology often originate from historical times, the term "paleoseismic studies" is commonly used in the literature. We hereby prefer to use the more general terms "field investigations" or "in-situ collected data" as an equivalent concept.

Information from field investigations can be used to identify earthquake effects on ancient constructions and/or the environment. However, pairing this information to a specific earthquake, known from historical records, is not a straightforward process. For instance, unless there is charcoal in the mortar of repairs (or coins, broken pottery) which one can radiocarbon-date, dating archaeological evidence is very difficult. Even more difficult is to prove that the cause was indeed a seismic event (and not other natural phenomena or a siege or fatigue) and that the observed damage is not cumulative but was the result of a single event. Regarding geological evidence, as Marco and Klinger (2014) explain "a major uncertainty is related to dating because the commonly used methods in paleoseismic research, namely radiocarbon and luminescence, have large error margins and these need to be correlated with the often-uncertain dates of reported earthquakes. Commonly, the geologists who find evidence for past earthquakes look for records of historical earthquakes listed in catalogs whose dates fall within the geological dating ranges." When the radiocarbon data and the stratigraphy are analyzed with Bayesian statistics, the correlations can be expressed in terms of probability density functions (Bronk-Ramsey 2009). As demonstrated in the last column of Table 1, the correlation is often loose and the reported matches mainly reflect the historical records, which before the first millennium might be incomplete even for events associated with surface rupture (GEM).

Despite the aforementioned difficulties and limitations, evidence from field investigations can be of great value, if treated carefully. We have thus built

Table 1 Sumary of past field investigations around the Dead Sea Transform Fault Zone that confirmed historical events. Curly braces indicate confidence intervals; "σ" is the standard deviation (normal distribution). The correlation of the events in parenthesis is less certain. In the second to last column, italics font style indicates events that occurred outside our investigated zone (27 N–36 N, 31 E–39 E), while square brackets indicate that the event is considered spurious. The parameters of the events with assigned IDs (in bold) can be found in Table 4; the rest are listed in Appendices B and D. For the missing abbreviations, see Appendix A. All dates are AD, except where specified

Study	Location	Observations	Event ID or year of correlated event	Dating constraint
Ellenblum et al. 2015	Tell Ateret (N Sea of Galilee)	Trenches, archaeology	142 BC	143–142 BC
Reches and Hoexter 1981	Jericho fault (S Jordan Valley)	Trenches	**H31BC** **H747**	200 BC–200 700–900
Russell 1985	Palestine and NW Arabia	Archaeology	**H112**, *130*, **H363a** or **H363b**, **H418**, **H551**, **H659a** or **H659b**	Unspecified
Marco et al. 1997, Ellenblum et al. 1998	Tell Ateret (N Sea of Galilee)	Archaeology	**H1202**, (**H1759a**), (**H1837**)	> 1178
Klinger et al. 2000	Araba valley (Jordan)	Archaeology, outcrops	**(H1212)**, **H1458**	> 1174
Gomez et al. 2003	Serghaya fault (Lebanon, Syria)	Trenches, outcrops	**H1705** or **H1759a** or **H1759b**	> 1700
Meghraoui et al. 2003	Missyaf segment (NW Syria)	Trenches, archaeology	(**H115**)[1] **H1170**	100–750 {2σ} 700–1030 {2σ} 990–1210 {2σ}
Marco et al. 2003	Sea of Galilee	Archaeology	**H747**	650–750
Daeron et al. 2005 (Dae05)	Yammouneh fault[2]	Trenches	**H1202**	864–1400
Zilberman et al. 2005	Elat fault (S Araba Valley)	Trenches	**H1068a**	Unspecified
Marco et al. 2005	Jordan Gorge fault (N Sea of Galilee)	Trenches	**H1202** **H1759a**	1020–1275 {2σ} > 1415
Akyuz et al. 2006 (Aky06)	N Yammouneh fault (S Turkey)	Trenches	**H860** **H1408** *1872*	< 1018 1284–1478 > 1650
Nemer and Meghraoui 2006 (NeMeg06)	Roum fault	Trenches, outcrops	**H1837**	> 84
Haynes et al. 2006 (Hay06)	N Wadi Araba fault	Trenches, archaeology	**H634** **H659a** or **H659b** *873*[3] **H1068a** **H1546**	< 687 641–700 641–1115 900–1155 1515–1918
Daeron et al. 2007 (Dae07)	Yammouneh fault	Trenches	(**H347**)[4] **H1202**	30 BC–469 {2σ} 405–945 {2σ} 926–1381 {2σ}
Elias et al. 2007	Lebanon thrust fault	Outcrops	**H551**, **H1063**	Unspecified
Thomas et al. 2007	Aila (Aqaba, Jordan)	Archaeology	**H363a** or **H363b**	360–400
Nemer et al. 2008	Rachaya-Serghaya fault	Trenches, outcrops	**H1759a**, **H1759b**	1482–1740[5]
Altunel et al. 2009	Amik Basin (S Turkey)	Trenches, archaeology	**H1408** *1872*	1391–1442 1801–1888
Ferry et al. 2011	Jordan Valley fault	Trenches	**H747** **H1033**	560–1640 560–1640
Wechsler et al. 2014 (Wech14)	Jordan Gorge (JG) fault (N Sea of Galilee)	Trenches	[92 BC] or **H31BC**[6] or [33] *130*[7][8]	392 BC–91 {2σ} 137–206 {2σ} 165–236 {2σ}

Table 1 (continued)

Study	Location	Observations	Event ID or year of correlated event	Dating constraint
			H303[9]	250–310 {2σ}
			H347[10]	269–329 {2σ}
			H363a or **H363b**[11]	294–369 {2σ}
			[500] or **H502** or **H551**	505–593 {2σ}
			H634 or **H659a** or **H659**[12]	619–684 {2σ}
Klinger et al. 2015 (Kli15)	S Wadi Araba fault	Trenches	**H363a**[11] or **H363b**	9 BC–492
			H747[13]	671–845 (cracks)
			[13]	671–845
			(**H1033**)	806–1044 (cracks)
			H1068a	1003–1138
			H1212	1155–1269
			H1458	1434–1459
Langgut et al. 2016	Yavneh (Palestine)	Archaeology	**H659a** or **H659b**	Occurred in spring

[1] Possible match with H847 in West Syria or the event of the same year in Antioch.

[2] Dae05 assigned H1759a (foreshock) to the Rachaiya fault and H1759b to the longer Serghaya fault.

[3] Am94 argues that the event of 873 occurred in Saudi Arabia. Hay06 note that perhaps the event occurred in Wadi Arabia but it was not reported there because of lack of population. The latter scenario matches better with the distribution of active faults in the area.

[4] Dae07 note that the deformation might have formed due to the previous event. If that is not the case then possible matches could be H455, H551, H847, and H860, with the latter being the most probable since Aky06 have correlated it with the North Yammouneh fault.

[5] The dates are drawn from a figure and thus may not be highly accurate.

[6] The events of 92 BC and 33 are spurious according to Am09. Therefore, Wech14 probably identified H31BC.

[7] The year 130 is out of the range of the sample of Wech14. Am09 argues that in fact the event of 130 occurred in North Turkey. The finding of Wech14 probably relates to an event absent from the catalogs.

[8] This event appears to be absent from the catalogs.

[9] According to historical sources, the epicenter of H303 was along the Lebanese coast in north of Sydon. Wech14 identified the event in North Sea Galilee (250–310; 2σ). For both historical and geological evidence to be valid, the earthquake must have ruptured a fault between Sea of Galilee and Beirut, passing east of Mountain Hermon. That description matches with the trace of the Roum fault. It is unclear whether the Roum fault reaches Beirut and connects with the Lebanon thrust fault (NeMeg06).

[10] See §5.4.

[11] Kag11 argues that H363a occurred in North Palestine and H363b further south. Therefore, Wech14 probably identified H363a and Kli15 H363b.

[12] None of the three candidate events appears to have occurred close to the Sea of Galilee (Lake Tiberias). The event that Wech14 identified might be absent from the catalogs.

[13] Kli15 found geological evidence in the South Wadi Araba fault that can be correlated with two events between 746 and 757: one that happened further North (hence only small cracks found) and one that ruptured Wadi Araba fault. While the former might be H747, the second event is probably absent from the catalogs. There is supporting evidence of multiple events between 746 and 757 that damaged Palestine, since the dates of the primary sources are very inconsistent (§5.4). Alternatively, this event happened in the first half of the ninth century, forming a seismite in the Dead Sea lake (Table 2).

upon the work of Marco and Klinger (2014) and Kagan et al. (2011) (Kag11), who reviewed such studies along the DSTFZ, in an attempt to validate the inevitably incomplete historical data (Tables 1 and 2). The next two sessions summarize the findings of such previous field investigations. The analyzed data were later used to constrain the plethora of quantitative estimations available in the existing parametric catalogs.

4.2.1 Fault trenches and archaeology

Parametric catalogs are usually affected by large uncertainty in location and magnitude solutions. Excavating trenches across active faults and analyzing the observed displacements can associate an event with a specific fault segment, thus constraining the earthquake's location. Assuming that the rupture did not propagate to other segments, one can also infer the earthquake's magnitude from empirical scaling relations that use the fault's geometry (e.g., area, length). Some relations (e.g., Anderson et al. 1996) use also the fault's displacement during the event, which may be inferred from geological or archaeological investigations. Moreover, in few cases, lack of in situ evidence can endorse suspicions that a reported event is in fact spurious or simply prove that its rupture did not reach the segment in question.

Table 1 presents a list of past field investigations around the DSTFZ that, according to their authors, confirmed historical events. The table illustrates the rather loose dating constraint behind the correlations, in particular regarding archaeological data. We re-evaluated these correlations, based on the current state-of-knowledge. New historical or geological evidence have emerged since some of these studies were published, shedding light to alternative interpretations of the results.

4.2.2 Seismically triggered soft-sediment deformation structures

Seismically triggered soft-sediment deformation structures (SSDS), i.e., seismites, are formed when layered deposits at the lakebed/seabed are deformed by ground shaking; the sediments get fluidized, brecciated, re-suspended, and then re-settled in their new deformed structure (Marco et al. 1996; Agnon et al. 2006). The same procedure can be also triggered by the presence of long water waves (i.e., seiche or tsunami), which mix the stratified lakebed/seabed (Agnon et al. 2006). The age of a seismite is usually interpolated from the radiocarbon age-depth data of organic remains (e.g., wood) using stratigraphic constraints and annual laminae counting. The resulting modeled calendar age of a seismite is in the order of decades (68% confidence interval, 1 standard deviation σ) to few centuries (95% confidence interval, 2σ). The dating range can be further narrowed by the superposition principle and rate of sedimentation (Ken-Tor et al. 2001b). The latter also allows the age determination of layers that lack organic debris and thus cannot be dated with radiocarbon. It is important to note that a uniform deposition rate may be an oversimplification for the arid climate of the Dead Sea, which often features irregular flash floods (Agnon et al. 2006; Lopez-Merino et al. 2016).

Ken-Tor et al. (2001a) (Ken01) and Kag11 analyzed samples from the Dead Sea lake (DSL), directly comparing modeled radiocarbon ages of the soft-sediment deformation structures that they identified with the historical records to check for possible correlations. We used their findings in our analysis. For reasons explained in the Appendix C2, we did not use the results from a similar study that Migowski et al. (2004) (Mig04) performed, even though we listed them in Table 2.

As far as the DSL is concerned, SSDS that are well classified as seismically triggered could indicate whether a historical event did occur in the region or not and perhaps provide a rough indication about its size given its distance. The logic behind the latter is that the energy that reached the sampled site has to be enough to cause either direct disturbance in the stratification of the lakebed or a seiche. Several source and propagation effects play a role in that. Kag11 note that the formation of seismites depends on water depth at the site (mass of water above sediment), lithology, sediment compaction, sedimentation rate, and the topography ("basin effect"). That is probably why Ken01 found no relationship between seismite thickness and historical earthquake intensity. Nevertheless, some empirical considerations can be made. In the absence of a seiche, the formation of seismites involves fluidization, which requires stronger ground shaking than liquefaction (Lowe 1975). Atkinson (1984) set the magnitude threshold for the latter at M 5, based on ground motion duration considerations. Similarly, one could reasonably assume that MSK intensity around VIII ("[…] large cracks and fissures opening up, rockfalls […]") should have been

Table 2 Multisite comparison of Holocene seismites from four lacustrine sediment samples along the Dead Sea lake (DSL). Curly braces indicate confidence intervals; "σ" is the standard deviation (normal distribution) and bold deformation values indicate correlation within the 1σ range. In the column on the left, italics font style indicates events that occurred outside our investigated zone (27 N–36 N, 31 E–39 E), while square brackets indicate that the event is considered spurious. MSK_{DSL} is the expected MSK intensity at DSL, given magnitude and distance from the epicenter R_{DSL}. The study sites are shown in Fig. 1. The parameters of the events with assigned IDs (in bold) can be found in Table 4. For more information about the events and the missing abbreviations, see Appendices A, B, and D. All dates are AD, except where specified. A more detailed version of this table is available in Appendix C3

Event ID or year of correlated event	Event parameters	Study/site				Remarks
		Ken01 Ze'elim	Mig04 Ein Gedi	Kag11 Ze'elim	Kag11 Ein Feshkha (EF)	
–				140 BC–66 BC {1σ}	146 BC–96 BC {1σ}	This event is either absent from catalogs or is [139 BC]
[92 BC]			✓		126 BC–76 BC {1σ}	Am09 and Kar04: spurious event
–					101 BC–42 BC {1σ}	H31BC already correlated in EF, so this event is absent from catalogs
69 BC	R_{DSL} = 500 km	200-60 BC {1σ}[1]	✓[2]		96 BC–41 BC {1σ}	Agn06[1]: relates to [139 BC]; masked by subsequent deformation[2]
H31BC	MSK_{DSL} = VI	40 BC–130 AD {1σ}	✓	40 BC–35 AD {1σ}	57 BC–7 AD {1σ}	
[33]		64 BC-311[3,4]	✓	12–91 {1σ}	25–100 {1σ}	Am09: spurious event; alternative match[3]: **H112**; dated based on sedimentary rate[4]
H76	MSK_{DSL} = III		✓			Very low MSK_{DSL}
[90]			✓			No historical record
H112	MSK_{DSL} = VI	[3]	✓	[5]		Am09: only archaeological evidence
H115	MSK_{DSL} = III		✓	55–210 {1σ}[5]		Alternative match[5]: **H112** {1σ}
[175]			✓			No historical record
H347	R_{DSL} = 250 km				372–487 {1σ}[6]	Alternative match[6]: **H363a** or **H363b** {~1σ}
H363a or **H363b**	MSK_{DSL} > VI	358–580[7,8]			408–515 {1σ}[6,9]	Am09: seiche in DSL; Agn06[7]: relates to **H418**; alternative match[9]: **H418** {1σ}; dated based on sedimentary rates[8]
–					439–542 {1σ}[10]	Alternative match[10]: **H502** {1σ}
H418	R_{DSL} = 50 km	[7]	✓	386–519 {1σ}	448–551 {1σ}[9,11]	Alternative match[11]: **H551** {1σ}
[500]			Masked			Am09: Amalgamation of 4 events
H502	MSK_{DSL} = VI		✓	[12]	[10]	
H551	MSK_{DSL} = V		✓	467–606 {1σ}[12]	543–638 {1σ}[11,13]	Alternative match[12]: **H502**; alternative match[13]: **H634** {1σ}
H634	MSK_{DSL} = VII–VIII				603–692 {1σ}[13,14]	Alternative match[14]: **H659a** or **H659b** {1σ}
H659a or **H659b**	MSK_{DSL} = V–VI		✓		666–747 {1σ}[14,15]	Event outside the dating range; preffered match[15]: **H747** {1σ}
H747	MSK_{DSL} = VI		✓	699–848 {1σ}[17]	795–856 {1σ}[15,16]	Michael: Tsunami in Med., seiche in DSL; correlated rupture in Wadi Araba[16] (Table 1); Kag11[17]: **H747** or *757*. More likely the former
757					801–861 {1σ}[18]	*757* perhaps in NE Syria (INGV94); alternative match[18]: **H854** {1σ}
H847	MSK_{DSL} = III				849–905 {1σ}	Very low MSK_{DSL}; perhaps event absent from catalogs or **H854**
H860	MSK_{DSL} = III		✓		859–915 {1σ}	Very low MSK_{DSL}; perhaps event absent from catalogs
873	R_{DSL} = 600 km				885–939 {1σ}	Very large R_{DSL}; perhaps event absent from catalogs

Table 2 (continued)

Event ID or year of correlated event	Event parameters	Study/site				Remarks
		Ken01 Ze'elim	Mig04 Ein Gedi	Kag11 Ze'elim	Kag11 Ein Feshkha (EF)	
H956	MSK_{DSL} = I				963–1005 {1σ}[19]	Alternative match[19]: **H991** {1σ}
H991	MSK_{DSL} = IV		✓		991–1026 {1σ}[19,20]	Alternative match[20]: **H1033** {~1σ}
1033 Mar 6			Masked			Am09: Istanbul
H1033	MSK_{DSL} = VII		✓		1013–1051[20,21]	Tsunami in Acre (Am09); alternative match[21]: **H1047** {1σ}
H1042	R_{DSL} = 400 km		✓			
H1063	MSK_{DSL} = III		Masked		1028–1067 {1σ}	
H1068a	MSK_{DSL} = V		✓		1044–1084 {1σ}[22]	Tsunami in Mediterranean (Am09); alternative match[22]: **H1068b** {1σ}
1114 Nov 29	MSK_{DSL} = I		✓			Very low MSK_{DSL}
1138	MSK_{DSL} = II				1118–1155 {1σ}[23]	Alternative match[23]: **H1113** {~1σ}
H1170	MSK_{DSL} = IV–V				1150–1190 {1σ}	
H1202	MSK_{DSL} = V	[24]	Masked[25]		1199–1240 {1σ}[26]	Tsunami in Mediterranean (Am09); Agn06: masked[24], apparent not masked[25]; Kag11[26]: **H1202** or **H1212**
H1212	MSK_{DSL} = V–VI	1244–1385{1σ}[27]	✓		1199–1240 {1σ}[26]	**H1212**[27] outside modeled age range; perhaps event absent from catalogs
H1293	MSK_{DSL} = VII	1280–1390 {1σ}	✓		1260–1293{1σ}	
H1313	MSK_{DSL} < I				1300–1343 {1σ}	Very low MSK_{DSL}; perhaps event absent from catalogs
H1408	MSK_{DSL} = III		Masked			
H1458	MSK_{DSL} = VIII		✓	1400–1650[28]		Extrapolation from age-depth deposition model[28]
H1546	MSK_{DSL} = VI		✓			Tsunami in Gaza? (Am09)
H1588a	MSK_{DSL} = VI		✓			
1656	R_{DSL} = 2000 km		✓			Event too far away
[1712]			✓			Ami94: Epicenter in Jerusalem
H1759a or **H1759b**	MSK_{DSL} = V–VI		✓			
1822	MSK_{DSL} = II		✓			Very low MSK_{DSL}
H1834	MSK_{DSL} = VIII	1670–1950 {1σ}	Masked			
H1837	MSK_{DSL} = V		✓			Seiche in Sea of Galilee? (Am09)

The superscript numbers are used to connect the content of columns 3-6 to the notes in the last column (column 7).

reached in the DSL by a candidate event for the correlation to be valid. Using the DSTFZ-specific attenuation relation of Am06 and assuming reasonable values for the errors in magnitude and/or location (§5.3), a lower bound of MSK intensity V could be used. If the preferred magnitude and location of the candidate event result in MSK intensity below this threshold, then the correlation is unlikely.

Table 2 summarizes the findings of Ken01, Kag11, and Mig04, who examined samples for seismites in four locations collected from around the DSL. The corresponding earthquakes are listed as assigned by the authors. Additional metadata such as the preferred magnitude and location of the event, the seismite's thickness, and the 2σ dating range are available in a more detailed version of this table that can be found in Appendix C3. We re-assessed all the correlations proposed by these three studies given the current state-of-knowledge regarding the events in question and the specific dating constraints. In light of new studies, many of the proposed correlations in the literature correspond to seismic events that are either spurious or occurred too far away from the DSL to cause enough ground shaking for a seismite to be formed (e.g., *1822* or *1656*). Furthermore, several SSDS (e.g., H634 or H956) can be assigned to multiple events with similar statistical significance, given the uncertainty of the age-depth deposition models (Ken01; Fig. 3 in Kag11). The great number of field evidence regarding a number of possible earthquakes before 31 BC does not agree with the limited historical information we have about strong ground shaking in that time period. This indicates that the historical records before 31 BC might be mostly incomplete.

It is notable that only two historical events have been identified in all the samples (i.e., H31BC and 33 AD). The last one is in fact considered spurious by some modern sources (e.g., Am09). The absence of a seismite in the samples can often be explained even if an earthquake powerful enough to form a SSDS occurred nearby. Ken01 argue that the lack of well-known historic earthquakes in the Ze'elim archive coincides with site-specific periods of depositional hiatuses. The location of the Ze'elim terrace is sensitive to lake level fluctuations that induced hiatuses during low lake stands (Ken01, their Fig. 3b). We should point out however that the samples of Kag11 from the same area did include events between 400 and 800. Thus, as a general note, the results of seismite-related studies must be treated with caution. The existence or absence of correlated seismites is a good indication that the event is properly reported or not only when multiple sites provide the same

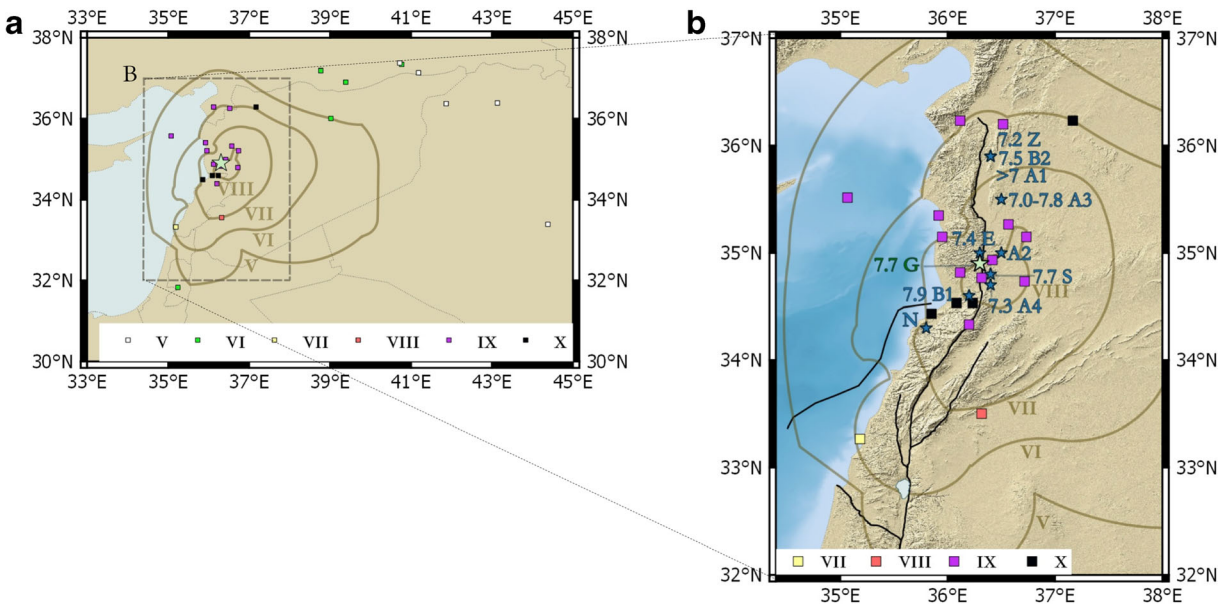

Fig. 3 The June 29, 1170 earthquake (H1170). The maps contain MCS macroseismic intensities (squares) (Guid04b; INGV05), MSK isoseismals (Am09), major fault traces, and original location and magnitude solutions in parametric catalogs. A1: Ambraseys and Barazangi (1989); A2: Am94; A3: Ambraseys and Jackson (1998); A4: Am06; B1: BM79; B2: BM91; E: EMME; G: Guid04b; H: Hough and Avni (2009); M: Meghraoui et al. (2003); N: NOAA; S: Sb05; Z: Zuhair et al. (2015)

conclusion; the correlation has a unique solution and falls within the 1σ range.

5 Data analysis

5.1 Magnitude homogenization

Modern earthquake catalogs use the moment magnitude scale (M_w) (Hanks and Kanamori 1979), which does not suffer from saturation effects and can also be related to the fault parameters. Unfortunately, most of the existing parametric catalogs for our zone use a variety of magnitude scales (Grigoratos et al. 2020), such as M_s (publications by Ambraseys; Sb05), local magnitude M_L (Ben-Menahem 1979), or equivalent magnitude (M_e, INGV94 and INGV05). As a result, the need of harmonization to a common magnitude scale was evident. Hence, M_s values have been converted to M_w using GEM's conversion equation (Eq. 1, Di Giacomo et al. 2015). GEM used a global dataset with more than 16,000 data points, orthogonal distance regression and the validity range goes up to magnitude 8.1. Concerning M_L, it is not possible to define a unique global relation connecting M_L to M_w, due to the agency-specific site and distance calibration factors. We considered best to use the conversion equation of EMME (Eq. 2), since it is fitted against data from the region in question (2271 data points up to magnitude 8.3). Regarding the equivalent magnitude, Guidoboni et al. (2004) consider it equivalent to M_w (Di Giacomo et al. 2015).

$$M_w = e^{a+b\cdot M_s} + c, 3.0 \le M_s \le 8.2, \text{ (Di Giacomo et al. 2015)}$$
$$\text{where } a = -0.222 \pm 0.043, b = 0.233 \pm 0.004, \quad c = 2.863 \pm 0.056 \tag{1}$$

$$M_w = 1.0136\, M_L - 0.0502, 4.0 \le M_L \le 8.3 \text{ (EMME)} \tag{2}$$

5.2 Source selection and ranking

In this study, we only consider unique tectonic events between 31 BC and 1900. We decided not to go earlier than the first century BC based on the conclusion of Ambraseys and White (1997) that the historical data in BC times are very incomplete. The missing seismites between 200 and 31 BC support that claim (Table 3).

Table 3 Indicative numerical representation of the uncertainty estimates within our catalog

	V (very large)	L (large)	M (medium)
Magnitude	< 1.00	< 0.75	< 0.50
Epicentral location	No constraint	< 100 km	< 75 km

Since the location of historical earthquakes is very uncertain and the primary sources were usually based in the main administrative centers of the historical times, we decided to investigate an extended zone that is wide enough to include events that might have been originally reported in Cyprus or East Syria and important historical cities (e.g., Alexandria, Palmyra), which hosted prolific writers (Fig. 1). Our list covers the geographical area defined by the boundaries 27 N–36 N and 31 E–39 E (Fig. 4).

Similarly to what EMEC, EMME, GEM, and the National Oceanic and Atmospheric Administration (NOAA; Dunbar 2009) have done, we relied on existing parametric data, i.e., dates, epicentral coordinates, and magnitude estimates, derived from previous studies. We did not perform any new macro-seismic analyses. That said, our study made an in-depth cross-examination of past historical records against field investigations, which is summarized in Fig. 2. We first analyzed the references listed in the "Historical data" section and created a preliminary earthquake catalog based primarily on historical records. From the list, we removed those events which are either not associated with any damage or associated with damage not explicitly linked to a particular earthquake. The latter check is important because sometimes, the observed effects were not earthquake-induced, but were rather caused by conflicts, rainfall-triggered landslides, storms, or structural fatigue. Almost all screened events were reported by multiple secondary sources. Therefore, the next step was to use the data from the regional field investigations to:

- check how well the historical reports from primary sources correlate with damaged localities identified by archaeological evidence (Table 1, e.g., H31BC, H747).
- check how well the historical reports from primary sources correlate with the reported macroseismic intensities in parametric catalogs. Identify possible exaggerations (e.g., event of 92 BC, H1063), amalgamation of events (e.g., event of 500, H747, H847) or attempts of contemporary writers to draw

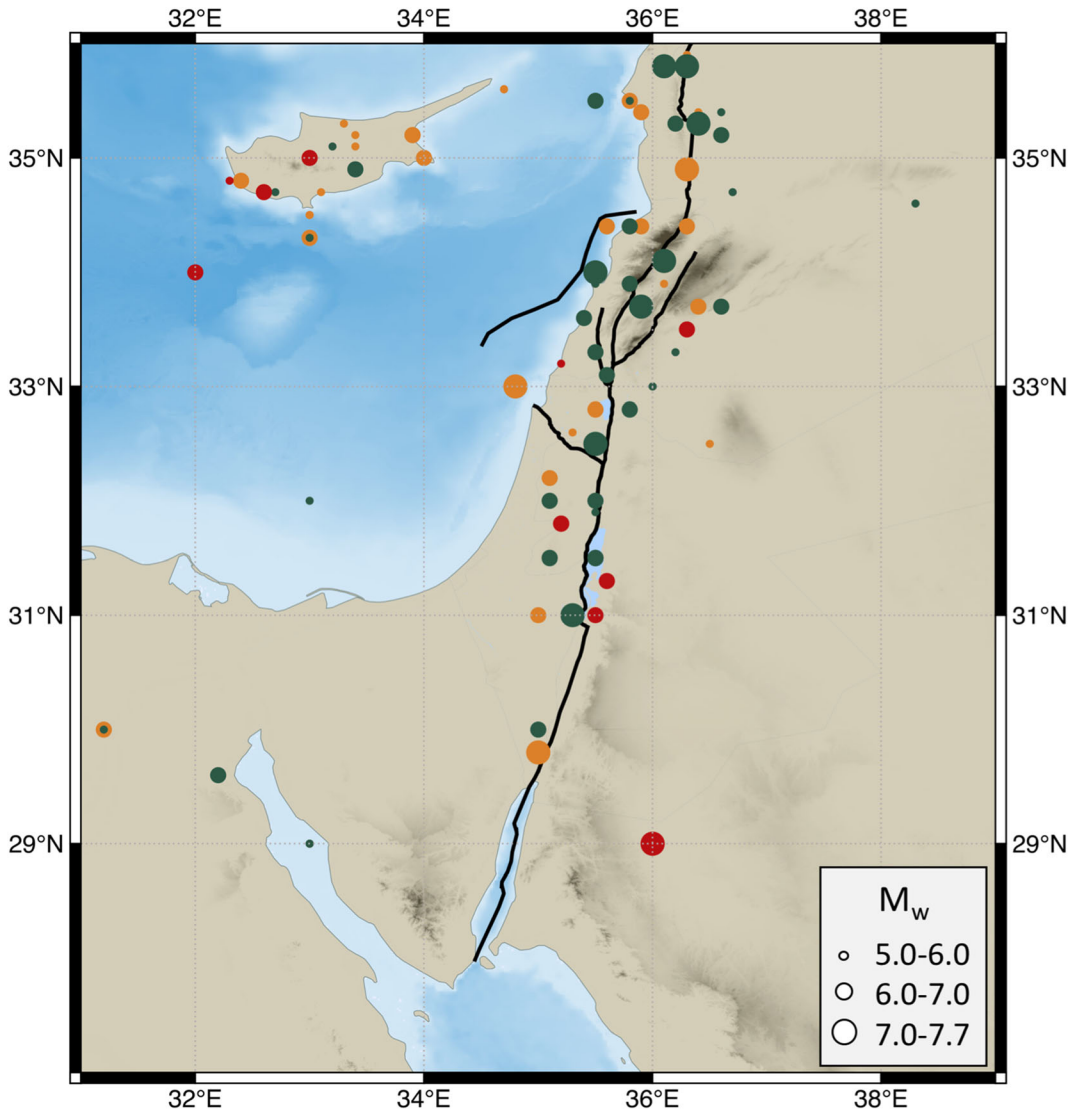

Fig. 4 Map with all the earthquakes with $M_w \geq 5$ between 31 BC and 1900 inside our investigated zone. The symbols are color-coded for LocUnc (Table 3), red for V, orange for L, and dark green for M. The black lines represent the major faults of the DSTFZ

theological and political morals from a natural disaster (e.g., 69 BC, 33, H1546).

- identify cases where the rupture propagated to neighboring segments (e.g., H31BC, H347, H363a, H1202).
- identify how the reported epicenter (e.g., H115, H860, H1170) and magnitude (e.g., H1293, H1546) correlates with the assigned rupture length using the scaling relations by Wells and Coppersmith (1994) (global) and Ambraseys and Jackson (1998) (region-specific). Next, use these results to narrow the range of available estimates. For a total number of 22 events, our selection of source for parametric values (epicentral coordinates and/or magnitude) was influenced by fault-related information (geometry, length).
- use the data from the seismite-related studies (Table 2) to check whether the event in question indeed happened at a reasonable distance from the DS lake. For example, the events of year 17 and of March 6, 1033 did not form any seismite. That is supporting evidence that they did not occur in Palestine but in West Turkey, as noted by several authors (e.g., Am09).

In case of lack of constraining field evidence, we had to critically evaluate the historical data in order to select

the most suitable location or magnitude. For several events, there were at least 4 different proposed solutions for the epicentral coordinates or the magnitude. There is a clearly larger availability of data for large magnitude events; for example, for H1170, there were 9 different location solutions and 10 different magnitude estimates proposed by different authors (Fig. 3). For most events, we referred not only to the modern descriptive catalogs but also to the primary (translated) sources as quoted in the books of Ambraseys and of INGV (i.e., INGV94 and INGV05). That enabled us to have our own critical view of parameters that were presented differently between catalogs. After reviewing all available information, we selected the solutions that were derived using the macroseismic intensity points that best reflect the most up-to-date analysis of the primary records. In few cases, the reported duration of the shock itself and the extent of the period of aftershocks provided an additional qualitative indication for its size (Salamon 2010).

We should point out that there were several events that were reported inside our investigated zone by some authors and outside by others. We reviewed all these events, but included in our catalog only those with preferred epicenter inside the investigated zone; that led several large events that occurred North of Antioch and had latitude larger than 36 N to be discarded.

Even though each event was analyzed separately, some common rules were applied to the parametric input data of the catalog. In descending order, the general hierarchy was (i) documents (co-)authored by Ambraseys; (ii) GEM; (iii) INGV; (iv) SB05; (v) EMEC; (vi) EMME; and (vii) Ben-Menahem. Exceptions to that rule were the epicentral locations provided by Am94 that were not derived from an isoseismal map and solutions listed in INGVweb that were computed using less than 3 data points. The magnitude type was not considered as a criterion in our selection process since the uncertainty from conversion to moment magnitude is usually much lower than the uncertainty of the original estimates. The reasoning behind the aforementioned order was somewhat subjective, although driven by certain reasonable considerations. Ambraseys and INGV are specialized in this research field and their reports are based on primary sources, which they cite and quote. The latest book of Ambraseys (Am09) was written after both INGV books and thus the former often reviews and comments on the conclusions of the latter. As a result, Am09 was the selected source for the dating of almost all the events. At the global scale, GEM's procedure was very transparent, even though it was a compilation of previous estimates. In the regional domain, the epicentral coordinates and surface wave magnitudes computed by SB05 have been derived mainly from original isoseismal maps utilizing the nomograph of Shebalin (1970). On the contrary, EMEC and EMME were large-scale projects that relied on previous studies.

We should mention that our confidence in the magnitude estimations of Ben-Menahem varied depending on the input data he used for his calculations. The first reason is because he relied heavily on the catalog of Sieberg (1932), who often amalgamates different events, especially in North Syria. That is particularly crucial because Ben-Menahem often derived magnitude estimates using only the "radius of extremal human perceptibility" (Δ_f), defined as the "epicentral distance at which MMI = 3.5," without any evident intensity data constraint (e.g., H115, H528, H1033, H1068, H1042, H1287c). In other instances, it is not transparent how the magnitude was estimated since there are no reported MMI values nor any Δ_f values (e.g., H31BC, H713, H1063, H1160). In other cases, he used only the maximum observed intensity (assumed equal to epicentral) as input (e.g., H1157c, H1546, H1759b). The few estimates of Ben-Menahem that were calibrated on both maximum observed intensity and on Δ_f were ranked higher (e.g., H76, H860, H991). The type of input behind each estimate by Ben-Menahem is available in Appendix D. The methodology of Ben-Menahem (1979, 1981, 1991) in general leads to rather large magnitude estimates.

In the "Historical data" section (§4.1), we mention that both INGV catalogs (1994; 2005) have been merged into an online geo-referenced archive (Guidoboni et al. 2019) (INGVweb). The latter provides magnitude estimations and epicentral coordinates for all the events in INGV94 (absent from the hardcopy) and in INGV05 (absent from the hardcopy for events with very few intensity data). It should be noted that the coordinates in the book (INGV05) are given in degrees and minutes, while the online archive uses decimal degrees. Regarding the dating of the events and the affected localities, both books were very reliable. That said, our confidence on the results of INGV05 varied depending on the amount of sites with reported intensities; the "Boxer" method (Gasperini et al. 1999; Gasperini 2004) that INGV05 employed seemed to work much better with plentiful data (e.g., more than 8 mapped intensities). That should be more or less expected since the method has been validated against the much richer

Italian dataset. The 2004 version of the "Boxer" method yielded rather low magnitude estimates when the maximum MCS intensity was IX or higher, yet the number of mapped intensities was less than 6 (e.g., H1212, H1458). This scenario is common in the Dead Sea region where vast pieces of land used to be uninhabited or lack cultural centers. For the 1212 earthquake in particular, the estimated magnitude was only M_e 5.8, even though Eilat (epicenter), Cairo (> 350 km away), and Al-Karak (150 km away) had assigned MCS intensities IX–X, VIII, and VIII respectively. The latest implementation of the method has been designed to deal exactly with that situation (Gasperini et al. 2010).

Lastly, we should note that the magnitude values in online archive of Guidoboni et al. (2019) (INGVweb) do not always match the values listed in the book (INGV05), with the documentation for these changes to be lacking. We found 11 events in the online archive with modified M_e compared with the book, with differences ranging from 0.2 to 1.5 magnitude units. For example, the reported M_e for H1033 is 6.0 in the book and 7.3 in the archive, while for H1068a, it is 8.1 in the book and 7.2 in the archive. While small changes could be explained by a different calibration of the Boxer method (Rovida et al. 2016), some of the large magnitude differences are well outside the typical uncertainty ranges. We opted to report the latest magnitude solutions of Guidoboni et al. (2019) in Table 4 and in Appendix D, since they were usually more consistent with the values estimated by other authors.

5.3 Uncertainty estimation

Uncertainty estimations are a prerequisite for any input of a probabilistic analysis (Bommer & Scherbaum 2008). Errors in the magnitude or location of historical events have a large impact on the occurrence rates of a forecasting model (Panzera et al. 2011, Panzera et al. 2016), on the maximum magnitude and on the segmentation of the fault model (Mignan et al. 2015). Errors in location can affect the forecasted ground motion shaking in case of scenario-specific hazard assessment. The problem is equally significant when probabilistic approaches such as the smoothed seismicity models are selected (Hiemer et al. 2014). Errors in dating are not that important for large magnitude events with long return periods, unless the analysis is time-dependent (Field et al. 2015). Conversely, large dating errors could affect the results of the declustering procedure (Gardner & Knopoff 1974).

The uncertainty surrounding the epicenter and magnitude determination from historical macroseismic data in particular is a well-known issue (Cecic et al. 1996). We thus attempted to estimate the level of uncertainty carried by the parametric results of the previous studies that we compiled (Table 3). Although the analysis is somewhat subjective, we consistently adopted the following workflow in order to do the classification; the criteria are sorted below progressively from broad to stricter.

a. All primary sources agree on the date, felt area, and damage distribution. These are key indications that the historical reports come from a single tectonic event within our region.
b. The author of the parametric estimates used mapped macroseismic intensities and a suitable empirical relation to determine the epicenter and the size of the event (e.g., Am09, INGV05, Sb05) and not other proxies or expert opinion (e.g., Ben-Menahem, INGVweb).
c. The parametric estimates of the different studies that used refined methodologies are in agreement (e.g., H1759b, while H1068a and H1170 are counter-examples).
d. The estimated parameters are consistent with any available evidence from field investigations. If the event has been associated to a fault, then we checked if its estimated epicenter is close to that fault (e.g., H363a, H551, H1068a, H1157c, H1170, H1202) and whether the estimated magnitude is within the range that geologists have assigned to this fault or specific rupture (e.g., H115, H363a, H551, H1068a, H1212). If the dip and width of the fault were known, then we used the projection of the fault plane instead of the fault trace.
e. The value of the estimated magnitude itself. The smaller the magnitude, the smaller the maximum distance between the event and a site with reported damages. For example, according to the global empirical formula of Ambraseys (1992) for M_s 6, the MSK intensity gets below V (slight damage to a few poorly constructed buildings) at distances > 75 km. The values using the DSTFZ-specific formula of Am06 are similar. As a result, it is highly unlikely that an event with magnitude around 6 or less will have an error in its epicenter of more than

about 75 km. We should note, however, that the large magnitude uncertainty in many events rendered this criterion inapplicable.

The considerations made for selecting the indicative thresholds in Table 3 follow, starting with the magnitude. Sb05 and Ben-Menahem do not provide any uncertainty estimates. Ambraseys' empirical relations have been assigned with an uncertainty of 0.3 in terms of magnitude (Am06). Guidoboni et al. (2004) have used the "Boxer" method for H1170 with intensity data from 29 locations (Fig. 3); they reported a mean magnitude of 7.7 with a 0.22 uncertainty. The global relation of M_s to M_w that GEM derived using more than 16,000 events yields an uncertainty of 0.36 for a magnitude 8 event (Di Giacomo et al. 2015). Given that M_s is a better proxy to M_w than any macroseismic intensity, the 0.22 value of Guidoboni et al. (2004) seems underestimated. Even though INGV05 has also used the "Boxer" method to compute all estimated magnitudes, unfortunately, no uncertainty values are reported in order to have a better idea of the overall uncertainty bounds and sensitivity. The uncertainty behind magnitude estimates derived from macroseismic intensities is expected to be rather large since the empirical relations do not take into account site effects (Sun et al. 1998) and the seismic vulnerability of the building population (Molin 1995). Although the relations have been derived using macroseismic data after the year 1900, they are applied to a time period of 2000 years, in which the construction practice has evolved dramatically. Another major and often understated assumption that complicates the estimation of the true uncertainty is that the intensity data are complete. If new mapped intensities are to be identified in historical documents or archaeological sites, then the resulting parametric estimates will obviously change. New refined procedures have been proposed in order to address this issue (Pasolini et al. 2008; Gasperini et al. 2010). With all the above in mind, we do not expect the magnitude uncertainty to be lower than 0.5. The next two thresholds were set arbitrarily as 150% and 200% of the first one respectively (Table 3).

Regarding the uncertainty in epicentral coordinates, Guidoboni et al. (2004) reported 100 km maximum uncertainty in the determination of the epicenter of H1170 (Fig. 3). The value of 100 km may seem at first glance large for such well-reported event. However, epicentral locations provided by modern local seismic networks often happen to be more than 50 km apart (Bratt & Bache 1988). We therefore chose the value of 100 km as the threshold for well-reported large events (Table 4). We were confident that the uncertainty was lower (i.e., < 75 km) only if the magnitude was smaller than 6 or the assigned epicenter was validated by the location of the associated fault. Even for a M_w 7.7 event (maximum in our catalog), the scaling relations (Wells & Coppersmith 1994; Ambraseys & Jackson 1998) give a rupture length of about 150 km, meaning that the epicenter cannot be more than about 75 km away, assuming strike-slip focal mechanism. Indeed, almost all the faults in the region are strike-slip and therefore the assumption that the epicenter is not far from the fault trace is valid.

5.4 Discussion on specific events

In this section, we analyze few controversial events that could potentially affect significantly the seismic hazard along DSTFZ. We first summarize the most up-to-date information and, when available, present new interpretations that our analysis revealed. All abbreviations and a more comprehensive list of our considerations regarding the rest of the events in our catalog can be found in Appendices A and B. Figure 1 shows the location of several key toponyms.

H347: According to historical sources, the epicenter of H347 was in Beirut. Dae07 and Wech14 identified the event east of Beirut, in the Yammouneh and Jordan Jorge segments respectively (Table 1). The correlation by Wech14 is rather poor since the date of the event is outside the 2σ range. The evidence has been found in two investigated fault sites about 130 km away, indicating a very long rupture, compatible with a magnitude (M) of 7.4–7.6 event (Wells & Coppersmith 1994; Ambraseys & Jackson 1998). However, the historical data does not necessarily support such a large size. The only primary source for this event is Theophanes (eighth century), who mentions that most of Beirut was destroyed; he does not reference any other affected localities. BM79 has assigned M_L 7 to this event based only on the maximum observed intensity (assumed equal to epicentral intensity); he cites Willis (1928), Sieb32, and Plassard and Kogoj (1981). Sieb32 is the only one who mentions a tsunami further north in Tablus, but he does not cite his source. INGVweb has assigned M_e 5.8, based probably only on the maximum observed intensity (Sibol et al. 1987). It is very hard to estimate the magnitude of the event because even

though the maximum observed intensity is large, only one affected city is mentioned. We preferred to use the more conservative estimate, i.e., M_L 7, which we then converted to M_w. This event requires further research.

H363a and H363b:Am09 concludes that two events happened the same day (May 19, 363) with a difference of 6 h, contrary to Am06 who assigned a single M_s 7.4 event. Sb05 and INGV94 also considered only one event. The two earthquakes caused the destruction of 22 towns in Palestine and West Syria. It is very hard to separate the effects of the two shocks and the issue of damage accumulation has to be noted. Furthermore, several sources amalgamate the effects of these events with those of a large earthquake in the Hellenic arc in 365.

Kag11, in agreement with Kli15, argue that H363a occurred in North Palestine and H363b further south. The rest of the field evidence are rather inconclusive. Wech14 assigned a sample from the Jordan Gorge fault (North Palestine) to the year 363; however, the match is outside the 1σ range. Ken01 have correlated a seismite in DSL with H363a or H363b or H418, while Agn06 argue that in fact it matches best with H418 (Table 2). A seismite that Kag11 have assigned to H347 correlates with greater statistical significance with either H363a or H363b (Table C.1). We should expect to find seismites associated with the shocks of year 363, since a seiche is reported in DSL (Am09).

H551: Eli07 attributed the July 9, 551, shock to the Lebanon thrust (offshore), thus explaining the origin of the destructive sea wave that is reported in the primary sources. It is very hard to comment on Eli07's dating scheme, since it was based on radiocarbon dating on vermetid samples, which were indicating that a shoreline-fringing bench suddenly emerged by about 80 cm (see their Data Repository). We should however mention an alternative scenario. Darawcheh et al. (2000), after analyzing the historical data attributed the event to the Roum fault. Wech14's evidence of rupture in the Jordan Gorge fault (dating range 505–593) supports Darawcheh et al.'s conclusion. The peak probability of Wech14's range is in year 551, which seems like a remarkable coincidence. The sea wave in that case can be explained by the slumping of part of the Libanus mountain called Lithoprosopon (Lebanon) in the sea, as Malalas reports. Am09 notes that the latter better explains the damage distribution along the coast, namely great damage near-field and rapid attenuation of the macroseismic intensities with distance. Goodman-Tchernov et al. (2009) found geological evidence of a strong tsunami in Caesarea (N Israel) that could be dated around the year 551.

Malalas (sixth century) and John of Ephesus (sixth century), both contemporary sources, date the event differently, September 550–August 551 and October 558–September 559 respectively (INGV94; Am09). The ranges are a result of the different dating schemes used in historical times. Am09 notes that although not impossible, "it would be odd for John to have multiplied a well-known earthquake in his own lifetime." However, they both describe very similar effects (i.e., coastal destruction, sea wave, aid from Emperor). Nevertheless, only Malalas mentions the slumping (rocksliding) of Lithoprosopon. We would like to highlight an important detail that previous catalogs have missed or neglected: John in fact mentions a second destructive shock that flattened Beirut probably several minutes or hours after the first one. He interprets the latter however as God's punishment against those who stole dead men's treasures; thus, we cannot be sure if it was indeed a severe aftershock.

Combining the current historical and in situ data leads to the following, plausible but far from definite, conclusion: a large earthquake ruptured the Lebanon thrust in 551 causing Lithoprosopon to fall into the sea, while a severe aftershock occurred on the Jordan Gorge fault. The latter would explain Wech14's field evidence and Rus85's claim that Pella (Tabqet Fahel, 50 km south of Jordan Gorge) was also damaged in the same year.

746–757: Michael the Syrian (twelfth century) has amalgamated at least three events between 740 and 757 into a single earthquake that presumably affected an area of about 600 km radius, from Egypt to Istanbul and from the east coast of the Mediterranean Sea to the Euphrates River in Iraq. Ambraseys (2005a) provides an extensive analysis arguing that Theophanes the Confessor, born a few years later, clearly mentions three events in Syria, Palestine, and Jordan between 746 (or 747) and 756 (or 757). For the debate over the exact dating of Theophanes, see Ambraseys (2005a). Kar04 has investigated the first two earthquakes. Some modern catalogs still report only one or two events in that decade.

We present below the key primary references in chronological order. Theophanes mentions an earthquake that affected Palestine, Jordan, and Syria on January 18, 746 (or 747). He mentions widespread damage just east of DSL. Later, Arab chronicles mention an earthquake in

May 4, 747–June 2, 748 in Jerusalem that was felt in Damascus. Other later chronicles indicate damage in Tiberias and Mount Tabor around that period. Dionysius of Tel Mahre (ninth century) mentions that the temple of Mabug (Manbij) collapsed in September 747–August 748. Archeological evidence indicates damage south of Sea of Galilee (Bet Shean) after a date ranging between August 748 and August 749. Later, Arab chronicles note an event between August 31, 748 and August 19, 749 which damaged the Al Aqsa Mosque in Jerusalem. Theophanes adds another event in early 749 (or 750) in Syria and Mesopotamia, where he mentions evidence of surface faulting. Dionysius of Tel Mahre notes that three villages collapsed in Khabura on March 3, 756, while Theophanes mentions a shock on March 9, 756 (or 757) in Syria and Palestine; he characterizes it "not small" (and not "powerful" as INGV94's translation from Greek states). Lastly, later, Arab chronicles report damage at the Al Aqsa Mosque in Jerusalem which was under repair at some point after 757.

Even though the evidence is rather inconclusive, we could identify at least three possible events: (i) in January 18, 747 in the Jordan Valley (H747), (ii) in 750 close to modern Manbij, and (iii) in March 757 near modern Al-Hasakah. The last two earthquakes fall outside our investigated zone and are thus not included in Table 4.

ReHo81 and Fer11 assigned H747 to the Jordan Valley fault system, Marc03 assigned it to a fault below the Sea of Galilee, while Am09 concluded that the event ruptured a fault that passes through Jerusalem, Tiberias, and Baalbek.

H1063: Am09 argues that Matthew of Edessa (twelfth century) exaggerated in his reports for personal reasons. The former also concludes that Antioch suffered no noteworthy damage and points out that aftershocks lasted only few days. Maximum intensity was reported in Tripoli (Lebanon), while Acre, Tyre, and Latakia suffered damages. INGV05 and Am09, contrary to Sieb32 and Sb05, do not mention Damascus. Sb05 assigned M_s 6.9 and INGV05 (with only 4 reported intensities) M_e 5.6. We believe that these values present the upper and lower bounds of the possible size of this event. The widespread damage indicates a large event, while the relatively low epicentral intensity and the very short duration of aftershocks indicate moderate size (Salamon 2010). The magnitude of the August 1063 event, in our opinion, remains an unresolved issue. We preferred to be on the conservative side and thus chose the value of Sb05.

H1170: The June 29, 1170 earthquake is probably the largest event within our zone (Fig. 3). Thirty towns and fortified sites, from Tyre (Sur) till Antioch, have reported damages. Tripoli was apparently destroyed with very few survivors, while Aleppo (more than 150 km to the North) also suffered severe damages and great loss of life. Even though INGV05 and Am09 agree on the affected localities, the assigned intensities by the former are, in general, significantly higher (Fig. 3). Palestine did not suffer any notable damage and the reports by Ben-Menahem regarding the effects of the event in Caesarea and Egypt are not confirmed by INGV05 and Am09. The aftershocks lasted up to 4 months (William of Tyre twelfth century), without causing further destruction. Guidoboni et al. (2004) examined the hypothesis that there were in fact two different events, one close to Tripoli and one in the Ghab basin, and concluded that all but one primary sources hint to a single event.

As far as the field evidence is concerned, Meg03 found geological evidence that correlates H1170 with the Missyaf segment (2σ range) and Kag11 have correlated this distant event with a seismite in DSL (1σ range). The latter, given the distance, hints towards a very large event. Indeed, all but one magnitude estimate are in the range of M 7.0–7.9; the M 6.6 value by Hough and Avni (2009) seems less probable.

6 Results

6.1 Homogenized parametric catalog

We analyzed and cross-examined the available historical, geological, and archaeological data, following the aforementioned methodology (§3; §5.2; Fig. 2) and compiled a parametric earthquake catalog with $M_w \geq 5$ between 31 BC and 1900 covering the Dead Sea Transform Fault Zone and East Mediterranean (Table 4). We homogenized all size estimates in the moment magnitude scale (M_w) (Hanks and Kanamori 1979), to render the catalog applicable for seismic hazard assessment.

The majority of the events are located in the part of DSTFZ which extends from the southeast part of Dead Sea lake till Antioch (Fig. 4). From those, 9 with $M_w \geq$ 7.0 have been associated with the DSTFZ branches that extend north of the Sea of Galilee, with the largest ones reported in 1170 (M_w 7.7, Fig. 3) and 1202 (M_w 7.7). The area below Antioch in particular appears to have been very active in historical times with several events

Table 4 Homogenized parametric earthquake catalog with $M_w \geq 5$ between 31 BC and 1900 in East Mediterranean and Dead Sea Transform Fault Zone (27 N–36 N, 31 E–39 E). Universal time is reported. Asterisks in the ID column indicate foreshock or aftershock. Loc, location; Unc, uncertainty (Table 3). For more information about the events and the missing abbreviations, see Appendices A, B, and the extended electronic version of the catalog (Appendix D). Appendix D includes also parametric values for minutes and seconds (when available)

ID	Date source	Year	Month	Day	Hour	Latitude	Longitude	Loc Unc	Loc source	M_w	M_w Unc	M source
H31BC	Am09	-31				32.0	35.5	M	BM79	6.3	L	Kar04
H17BC	Am09	-17				34.7	32.6	L	INGVweb	6.8	V	BM79
H76	Am09	76				35	33	V	INGVweb	7.0	V	BM79
H112	Am09	112				31	35	L	Am94	6.3	V	Am94
H115	Am09	115	12	13		35.8	36.3	M	AmJa98	7.4	M	Meg03
H303	Am09	303	4	2		33.6	35.4	M	INGVweb	6.6	L	INGVweb
H332	INGV94	332				35.2	33.9	L	INGVweb	6.6	V	INGVweb
H342	Am09	342				35.2	33.9	L	INGVweb	6.6	L	INGVweb
H347	Am09	347				33.9	35.8	M	[1]	7.0	V	BM79
H363a	Am09	363	5	19	1	31.5	35.5	M	Am06	6.5	M	Kag11
H363b*	Am09	363	5	19	7	31.5	35.5	M	Am06	6.5	M	Kag11
H375	Am09	375				34.7	32.6	V	INGVweb	6.4	L	INGVweb
H418	Am09	418				31.8	35.2	L	INGVweb	6.6	M	INGVweb
H455	Am09	455	9			34.4	35.9	L	INGVweb	6.2	L	INGVweb
H476	Am09	476				35.4	35.9	L	INGVweb	6.2	L	INGVweb
H502	Am09	502	22	8		33.0	34.8	L	Sb05	7.2	L	Sb05
H528	Am09	528	11	29		35.5	35.8	L	INGVweb	6.0	L	INGVweb
H551	Am09	551	7	9	8	34.0	35.5	M	Eli07	7.5	M	Eli07
H634	Am09	634				31.8	35.2	V	INGVweb	6.8	L	EMEC
H659a	Am09	659	6	7		32.2	35.1	L	INGVweb	6.2	V	INGVweb
H659b*	Am09	659	9			31.9	35.5	M	INGVweb	6.0	V	INGVweb
H747	Sb05	747	1	18		32.8	35.8	M	Am06	7.0	M	Am06
H847	Am09	847	11	24		34.4	36.3	L	Sb05	6.2	V	BM79
H854	Am09	854				32.8	35.5	L	INGVweb	6.5	V	EMEC
H857	Am09	857	4			28	31	V	Am94			
H860	Am09	860	1			35.5	35.8	L	INGVweb	7.0	M	Am06
H885	Am09	885	11			30.0	31.2	L	PoTa80	5.8	L	INGVweb
H950	Am09	950	7	25		30.0	31.2	L	PoTa80	6.5	L	EMEC
H956	Am09	956	1	5		34	32	V	Am94	6.2	L	INGVweb
H991	Am09	991	4	5		33.7	36.4	L	Sb05	6.7	L	BM91
H1033	Am09	1033	12	5		32.5	35.5	M	AmJa98	7.3	L	INGVweb

Table 4 (continued)

ID	Date source	Year	Month	Day	Hour	Latitude	Longitude	Loc Unc	Loc source	M_w	M_w Unc	M source
H1042	Am09	1042				34.6	38.3	M	INGVweb	5.6	V	INGVweb
H1047	Am09	1047				31.0	35.5	V	EMEC	6.5	L	EMEC
H1063	Am09	1063	8			34.4	35.6	L	INGVweb	6.9	V	Sb05
H1068a	Am09	1068	3	18		29.8	35.0	L	Zilb05	7.2	L	INGVweb
H1068b	Am09	1068	5	29		32.6	35.3	L	INGVweb	6.0	M	INGVweb
H1111	Am09	1111	8	31		30.0	31.2	M	INGVweb	5.4	L	INGVweb
H1113	Am09	1113	7	18		31.8	35.2	V	[2]	6.3	V	BM81
H1117	Am09	1117	6	26		33.2	35.2	V	INGVweb	5.8	L	INGVweb
H1151	Am09	1151	9	27		32.5	36.5	L	INGVweb	5.1	L	INGVweb
H1156*	Am09	1156	10	13		35.4	36.4	L	INGVweb	5.5	M	EMEC
H1157a*	Guid04a	1157	4	2		35.4	36.6	M	INGVweb	5.4	M	INGVweb
H1157b*	Am09	1157	7	13		35.2	36.6	M	Sb05	6.6	M	Sb05
H1157c	Am09	1157	8	12		35.3	36.4	M	Am06	7.2	M	Am09
H1160	Am09	1160				34.8	32.3	V	INGVweb	6.0	L	INGVweb
H1170	Am09	1170	6	29	3	34.9	36.3	L	Guid04b	7.7	L	Guid04b
H1202	Am09	1202	5	20		34.1	36.1	M	AmBa89	7.7	M	INGVweb
H1212	Am09	1212	5	1		30	35	M	Am06	7.0	M	Am06
H1222	Am09	1222	5	11	6	34.7	32.7	M	INGVweb	6.0	L	INGVweb
H1259	INGV05	1259	3	22		33.5	36.3	V	INGVweb	6.5	V	EMEC
H1284	Am09	1284				33.3	36.2	M	PoTa80	5.6	V	INGVweb
H1287a	Am09	1287	2	16		33.9	36.1	L	INGVweb	5.8	L	EMEC
H1287b*	Am09	1287	3	8		34.7	36.7	M	INGVweb	5.1	L	INGVweb
H1287c	Am09	1287	3	22		35.5	35.8	M	INGVweb	6.0	V	EMEC
H1293	Am94	1293	1			31.5	35.1	M	INGVweb	6.6	M	Am94
H1313	Am09	1313	2	27		30.0	31.2	L	Am94	5.8	V	BM79
H1339	Am09	1339	1			34.4	35.8	L	INGVweb	6.2	L	EMME
H1350	Am09	1350	7			34.8	32.4	L	INGVweb	6.4	L	INGVweb
H1354	Am09	1354				35.1	36.4	V	NOAA			
H1392	Am09	1392	4	13		35	33	L	INGVweb	6.0	L	INGVweb
H1404	Am09	1404	2	20		35.9	36.3	L	AmBa89	5.6	V	INGVweb
H1408	Am09	1408	12	29		35.8	36.1	M	Sb05	7.4	L	Sb05
H1458	Am09	1458	11	16		31.0	35.3	M	Am06	7.1	L	Am06

Table 4 (continued)

ID	Date source	Year	Month	Day	Hour	Latitude	Longitude	Loc Unc	Loc source	M_w	M_w Unc	M source
H1481	INGV05	1481	3	18	13	35.1	33.2	M	INGVweb	5.6	M	INGVweb
H1491	INGV05	1491	4	24	17	34.9	33.4	M	INGVweb	6.6	M	INGVweb
H1546	Am09	1546	1	14		32.0	35.1	M	Am94	6.1	M	AmKa92
H1567	Am09	1567	4	25		34.5	33.0	L	EMEC	5.3	L	EMEC
H1568a	Am09	1568	10	7		34.7	33.1	L	EMME	5.4	L	EMME
H1568b	Am09	1568	10	10		35.5	35.5	M	Sb05	6.1	M	Sb05
H1577	Am09	1577	1	28		34.5	33.0	L	BM79	6.0	L	BM79
H1588a	Am09	1588	1	4		29	36	V	Am94	7.2	M	Am06
H1705	Am09	1705	11	23		33.7	36.6	M	Sb05	6.9	M	Sb05
H1710	Am94	1710	8	27		29	33	M	Am94	5.7	M	Am94
H1718	Am09	1718	12	10		35.3	33.3	L	EMEC	6.0	L	BM79
H1735	Am09	1735	4	11		35	34	L	EMEC	6.3	L	EMEC
H1746	Am09	1746	7	5		33	36	M	EMEC	5.2	L	EMEC
H1753	Am09	1753	12	18		33	36	M	EMEC	6.0	V	EMEC
H1754	Am09	1754	10			29.6	32.2	M	Am94	6.6	M	Am94
H1756	Am09	1756	1	17		35.1	33.4	L	EMME	5.0	M	EMME
H1759a*	Am09	1759	10	30	1	33.1	35.6	M	AmBa89	6.6	M	AmBa89
H1759b	Am09	1759	11	25	17	33.7	35.9	M	AmBa89	7.5	M	Am06
H1764	Am09	1764	2	14		34.4	35.8	M	EMME	6.2	L	EMME
H1796	Am09	1796	4	26		35.3	36.2	M	Sb05	6.8	M	Sb05
H1814	Am09	1814	6	27		29	33	L	Am94	5.7	M	Am94
H1834	Am09	1834	5	26	11	31.3	35.6	V	BM79	6.3	L	BM79
H1837	Am09	1837	1	1	14	33.3	35.5	M	Am06	7.0	M	Am97
H1845	Am09	1845	2	21	3	35.2	33.4	L	EMME	5.0	L	EMME
H1850	Am09	1850	2	12	20	33.9	35.5	M	EMME	5.6	L	EMME
H1868	Am09	1868	2	20	1	32	33	M	Am94	5.7	M	Am94
H1879	Am09	1879	7	11		29	33	M	Am94	6.0	M	Am94
H1894	Am09	1894	1	13	0	35.6	34.7	L	AmAd93	5.7	L	AmAd93
H1896a	Am09	1896	6	29	20	34.3	33.0	L	AmAd93	6.5	L	AmAd93
H1896b*	Am09	1896	7	3	6	34.3	33.0	M	AmAd93	5.6	L	AmAd93

[1] We increased Kh00's longitude coordinates by 0.3 to better match Dae07's finding that the event ruptured the Yammouneh fault

[2] We decreased Zuh15's latitude coordinates by 0.7 to better match Am09's note that the event was a local shock close to Jerusalem

with $M_w \geq 6.8$, (e.g., H115, H1157c, H1408, H1796). Regarding the DSTFZ segmentation, several events that rupture the DSL segment seem to not propagate south to Wadi Araba (e.g., H1033, H1293, H1546) (Kli15). According to Masson et al. (2015), part of the relative displacement is accommodated along faults located west of Wadi Araba, in the Sinai Desert. On the other hand, the Jordan Gorge segment appears to be better connected with the DSTFZ branches in the North (e.g., H303, H1202) (Marc05, Dae07, Wech14).

We examined 244 events reported in previous catalogs, from which 115 have been identified as real events within our investigated zone and have been assigned with an event ID (Appendix D). From these 115 events, 9 have been flagged as either foreshocks or aftershocks (following Gardner & Knopoff 1974), 93 have $M_w \geq 5$ (Table 4), and 67 have $M_w \geq 6$ and 14 $M_w \geq 7$. Even though EMEC and INGVweb provide magnitude estimates down to magnitude 4.2 and 3.7, respectively, we decided not to present values below M_w 5 in Table 4, since such magnitudes are not well constrained by historical data and will in any case not pass the completeness analysis (§6.2). These low magnitude events are included in the more detailed electronic version of the catalog, which can be found in Appendix D.

When compared with EMME (Zare et al. 2014), given the same area and magnitude range, our catalog contains more than double the number of events, with 33 events of $M_w \geq 6$ present in our catalog being absent from EMMEs. As a result, the catalog update might have a significant impact in the seismic hazard estimates for large return periods. In comparison with EMEC, even though our catalog has only 4 events more (Table 5), it actually shares only 84 common events. From the 27 events which are different, 1 caused no damages, 12 were considered spurious, and the remaining 14 events from EMEC were re-assigned with epicenters which fall outside our investigated zone. The latter case was common, since several events occurred north of Antioch and at least 17 events have most probably occurred in the Mediterranean (Medit.), Turkey or East Syria (Table 6). The reasons were amalgamation with previous disastrous distant events, mistranslation of town names, or a tsunami originating from the Hellenic Arc (Am09). Finally, given the respective timeframes of EMEC and GEM, our catalog contains 15 events of $M_w \geq 6$ and 7 events of $M_w \geq 6.5$ absent from these catalogs respectively.

6.2 Completeness

The magnitude of completeness in an earthquake catalog is the minimum magnitude above which all earthquakes within a certain region are consistently reported. The most reliable historical records usually originate from contemporary chronicles, which inevitably can report limited time periods (e.g., Malalas, Theophanes). The rise or death of a prolific writer can affect the completeness of the historical data, similarly to how the installation or termination of a seismic network affects instrumental data. Same stands for the period range covered by historical catalogs. For example, the very detailed book of INGV05 covers the period 1000–1500. As a result, our catalog contains 19 events with reported $M_w < 5$ by INGVweb, all from that period and most of them from Egypt (Fig. 5).

The identification of historical earthquakes depends greatly on the density of populated localities in the region in question. That is why the assigned epicentral coordinates often correspond to the location of a cultural center, e.g., Jerusalem, Damascus, Antioch (Fig. 4), since most of the intensity information are documented there. Thus, much fewer earthquakes are reported in Wadi Araba,

Table 5 Comparison with other parametric catalogs. Only fully parameterized events (date, epicenter, and magnitude given) within our investigation zone are taken into account

Parametric catalog	INGVweb	INGV05	EMME	EMEC	GEM	NOAA	This study
Events within invest. zone	72	16	43	111	16	16	115
M range	3.7–7.7	4.9–8.1	5.0–7.5	4.2–7.3	6.6–7.7	5.9–7.6	3.7–7.7
Time span	31 BC–1500	1000–1500	33 BC–1900	300–1900	1000–1900	33 BC–1900	31 BC–1900
Common events with this study	71	16	40	84	16	13	-
Coverage	Medit.	Medit.	Middle East	Medit. and DSTFZ	Global	Global	E Medit. and DSTFZ

Table 6 Historical events after 31 BC that are erroneously associated with the Dead Sea Transform Fault Zone. All new assigned locations are based on Am09. For more information, refer to Appendix B

Year (AD)	Month	Day	Alleged location	Most probable location
17			Sidon	Asia Minor
130			Palestine	N Turkey
494			N Lebanon	E Turkey
717			S Turkey	E Syria
749/750			Palestine	Manbij (N Syria)
757	3		Palestine/W Syria	NE Syria
881			Acre	Hellenic Arc
963	5	12	Antioch	Hellenic Arc
1033	3	6	Lebanon	Istanbul
1114	8	10	Jerusalem	E Anatolia
1149			N Antioch	Iran
1303	8	8	E Mediterranean	Crete
1344	1	3	SW Syria	S Turkey
1537	1	8	Antioch	Egypt
1656			Tripoli (Lebanon)	Tripoli (Libya)
1752	7	21	NE Syria	Italy
1802			Lebanon	N Aleppo

Egypt, or west of DSTFZ (zone 1), where the population was sparser. There, the little data are assumed complete only for $M_w \geq 7$ (GEM; Kli00). Based mainly on historical considerations, we determined more detailed completeness periods (Fig. 5) for the part of DSTFZ, which extends from the southeast part of DS lake till Antioch, plus Cyprus (zone 2). The improved completeness after year 1000 is endorsed by trenches along the DSTFZ, which have not identified any missing events within zone 2 in the second millennium (Table 1), and by the seismite-related evidence (Table C.1). The arrival of the Crusaders around 1100 improved the quality and coverage of the reports significantly, as shown by the smaller magnitudes present in Fig. 5.

7 Concluding remarks

The present study aimed at presenting an updated historical earthquake catalog (31 BC–1900; $M_w \geq 5$; Table 4) for the Dead Sea Transform Fault Zone (DSTFZ). Together with the updated instrumental catalog for the region (Grigoratos et al. 2020), these two publications offer nearly 2050 years of homogenized historical earthquake data, tailored for use in seismic hazard assessment studies (e.g., Grigoratos et al. 2018b).

The identification of historical events is a rather multi-disciplinary procedure that combines historical and cultural knowledge, engineering judgement, seismological background, and interpretation of geological evidence. The present study tries to address this complex task systematically (Fig. 2, §5.2), by cross-examining the historical, archaeological, and geological data (i.e., trenches, seismites).

While examining the reported correlations between historical records (§4.1) and geological evidence of past ruptures (§4.2), we observed the often rather poor dating constraint provided by trenches in coarse-grained sediments outside the Dead Sea, i.e., with an uncertainty of more than two centuries. Correlation of archaeological evidence with past reported events is even more uncertain (up to thousands of years), if not specified at all (Table 4). We also reappraised all previous correlations between seismically triggered soft-sedimentary deformation structures (seismites) in the Dead Sea lake and historical records (Table 2, Appendix C2), given the current state-of-knowledge behind each reported event and the specific dating constraints accompanying each seismite (Ken-Tor et al. 2001b; Kagan et al. 2011). The analysis indicated that seismite-related findings must be treated with caution and have greater value as supporting evidence rather than stand-alone proof.

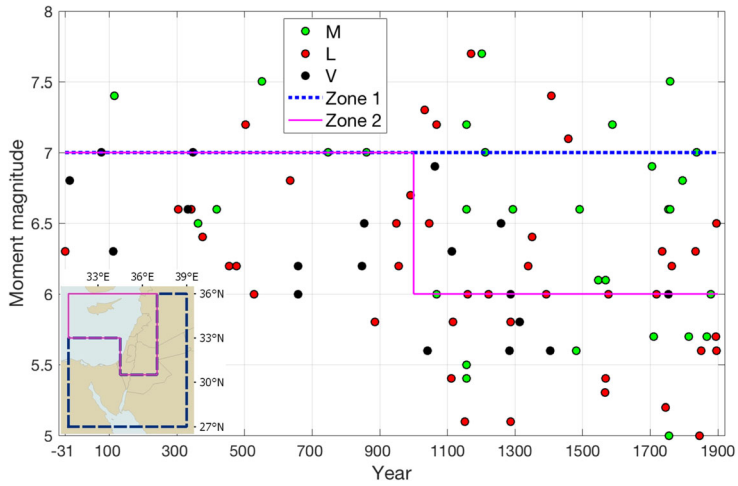

Fig. 5 Distribution of historical earthquakes in terms of time and size within our investigated zone. The lines (dashed blue for zone 1, magenta for zone 2) indicate the magnitude of completeness through time, while the color of the circles represents the uncertainty in M_w, as defined in Table 3

We should note that trenches along the DSTFZ and seismites in the Dead Sea lake hint to about 14 different and potentially significant events between the second century BC and fourteenth century AD that are missing from the historical records. The trenches (Table 1) in particular indicate that three missing events have occurred along the Jordan Gorge fault and one (perhaps in the first half of the ninth century, Table 2) in Wadi Araba. The remaining 10 possible events, inferred by uncorrelated SSDS (Table 2), are harder to interpret.

Our catalog contains 33 and 15 events of $M_w \geq 6$ that are not listed in Zare et al. (2014) and EMEC respectively. Compared with GEM's historical catalog (Albini et al. 2014), our compilation has 7 additional events of $M_w \geq 6.5$. The impact of these differences in the seismic hazard estimates for long return periods might be significant. The majority of the earthquakes in our list are located in the part of DSTFZ, which extends from the southeast part of Dead Sea lake till Antioch, and in Cyprus. There, the catalog was found complete down to M_w 6 since about the year 1000. The whole catalog is considered complete down to M_w 7 since 31 BC. As a matter of fact, 9 earthquakes with $M_w \geq 7.0$ have been associated with the DSTFZ branches that extend north of the Sea of Galilee (Fig. 4), with the largest ones reported in June 1170 (M_w 7.7, Fig. 3) and May 1202. We should note that 17 events reported in previous catalogs as having occurred around DSTFZ, most probably occurred in the Hellenic Arc, Turkey or east of Syria (Table 6).

In the "Uncertainty estimation" section, we estimated the uncertainty carried by the parametric results of the previous studies that we compiled (Table 4). Even though this procedure is somewhat subjective, we introduced a basic classification system to facilitate the process. We argue that the uncertainty will probably be around 0.5–1.0 for M_w and 75 km–100 km for the epicentral location, decreasing with richness of data and increasing with magnitude size.

As far as the analysis of specific controversial events potentially impacting the regional seismic hazard is concerned (§5.4), combining the primary historical transcripts and up-to-date in situ data indicates that probably a large earthquake ruptured the Lebanon thrust (offshore) in 551 causing mountain Lithoprosopon to fall into the sea, with a severe aftershock possibly occurring few hours later on the Jordan Gorge fault. Regarding the 746–757 sequence, even though the evidence is rather inconclusive, we could identify at least three possible events, from which only one is within our investigated zone.

The analysis of the translated original sources revealed that some events cannot be resolved unless new historical evidences come to light. For example, it is still unclear whether a large earthquake struck Syria and Judea in 1182 (Appendix B), as reported in modern parametric catalogs. Moreover, additional data are necessary in order to re-evaluate the size of H347, H1042, and H1063 or assign magnitude values to H857 and H1354, which at the moment lack this parameter. Unresolved are also locations of H1354 and of H1588a, due to missing information and sparsely populated epicentral region respectively (Appendix B). It is also still unclear whether a large earthquake struck Jerusalem in the year 33, as some religious sources and geologic evidence suggest (Williams et al. 2012; Table 2). In general, the re-assignment of macroseismic intensities (in a unified scale) and the computation of new magnitude estimates would benefit almost

all events in the region. Although critical, this task was outside the scope of the present study. Another future perspective could be to try to assign depth values to the events, taking into account the attenuation of intensities with distance and the total seismogenic depth. Even though there are some algorithms for that (e.g., Gasperini et al. 2010), the resulting values are usually underestimated. Further research is required also on defining a ground motion threshold below which the formation of seismites should not be expected. As a first-order approximation, we introduced the MSK intensity level VIII, which considering the uncertainty in magnitude and location could go down to MSK V.

Acknowledgments We are grateful to Ricardo Monteiro and Paola Ceresa for several stimulating discussions, which motivated the work described in this paper. We thank Jefferson Williams for reading an earlier version of this manuscript.

Funding information The first author was funded by the Doctoral Program of the University School of Advanced Studies IUSS Pavia (Italy). The fourth author received a scholarship from the Erasmus Mundus Masters in Earthquake Engineering and Engineering Seismology Consortium (MEEES).

References

Agnon A, Migowski C, Marco S (2006) Intraclast breccias in laminated sequences reviewed: recorders of paleo-earthquakes. Geol Soc Am Spec Pap 401:195–214

Akyuz HS, Altunel E, Karabacak V, Yalciner CC (2006) Historical earthquake activity of the northern part of the Dead Sea Fault Zone, southern Turkey. Tectonophysics 426(3):281–293

Albini P, Musson RM, Rovida A, Locati M, Gomez Capera AA, Vigano D (2014) The global earthquake history. Earthquake Spectra 30(2):607–624 https://emidius.eu/GEH/map.php

Albini P, Antonucci A, Locati M, Rovida A (2018) Should users trust or not trust Sieberg's Erdbebengeographie (1932)? Seismol Res Lett 90(1):335–346

Aldersons F, Ben-Avraham Z (2014) In: Garfunkel Z, Ben-Avraham Z, Kagan E (eds) The Seismogenic thickness in the Dead Sea area, Dead Sea Transform Fault System: Reviews. Springer

Altunel E, Meghraoui M, Karabacak V, Akyuz SH, Ferry M, Yalciner CC, Munschy M (2009) Archaeological sites (tell and road) offset by the Dead Sea fault in the Amik Basin, southern Turkey. Geophys J Int 179:1313–1329

Ambraseys N (1962) A note on the chronology of Willis's list of earthquakes in Palestine and Syria. Bull Seismol Soc Am 52(1):77–80

Ambraseys N (1992) Soil mechanics and engineering seismology. Proc. 2nd Natl. Conf. on Geotech. Eng., (invited paper)

Ambraseys N (2001) Reassessment of earthquakes, 1900–1999, in the Eastern Mediterranean and the Middle East. Geophys J Int 145(2):471–485

Ambraseys N (2005a) The seismic activity in Syria and Palestine during the middle of the 8th century; an amalgamation of historical earthquakes. J Seismol 9(1):115–125

Ambraseys N (2005b) Historical earthquakes in Jerusalem – a methodological discussion. J Seismol 9(3):329–340

Ambraseys N (2006) Comparison of frequency of occurrence of earthquakes with slip rates from long-term seismicity data: the cases of Gulf of Corinth, Sea of Marmara and Dead Sea Fault Zone. Geophys J Int 165(2):516–526

Ambraseys N (2009) Earthquakes in the Mediterranean and Middle East: a multidisciplinary study of seismicity up to 1900. Cambridge University Press

Ambraseys N, Barazangi M (1989) J Geophys Res Solid Earth 94(B4):4007–4013

Ambraseys N, Jackson J (1998) Faulting associated with historical and recent earthquakes in the Eastern Mediterranean region. Geophys J Int 133(2):390–406

Ambraseys N, White D (1997) The seismicity of the eastern Mediterranean region 550-1 B.C.: a re-appraisal. J Earthquake Eng 1:603–632

Ambraseys N, Melville CP, Adams RD (1994) The seismicity of Egypt, Arabia and the Red Sea: a historical review. Cambridge University Press, Cambridge

Amiran DHK (1950) A revised earthquake-catalogue of Palestine. Israel Explor J 1(4):223–246

Amiran DHK (1952) A revised earthquake-catalogue of Palestine. Israel Explor J 2(1):48–65

Amiran DHK, Arieh E, Turcotte T (1994) Earthquakes in Israel and adjacent areas- macroseismic observations since 100 B.C.E. Israel Explor J 44(3/4):260–305

Anderson JG, Wesnousky SG, Stirling MW (1996) Earthquake size as a function of fault slip rate. Bull Seismol Soc Am 86(3):683–690

Atkinson G (1984) Simple computation of liquefaction probability for seismic hazard applications. Earthquake Spectra 1:107–123

Ben-Menahem A (1979) A new earthquake catalogue for the Middle East, 92BC-1979AD. Boll Geofis Teoret Appl 21: 245–310

Ben-Menahem A (1981) Variation of slip and creep along the Levant Rift over the past 4500 years. Tectonophysics 80(1–4):183–197

Ben-Menahem A (1991) Four thousand years of seismicity along the Dead Sea rift. J Geophys Res Solid Earth 96(B12): 20195–20216

Bommer JJ, Scherbaum F (2008) The use and misuse of logic trees in probabilistic seismic hazard analysis. Earthquake Spectra 24(4):997–1009

Bratt SR, Bache TC (1988) Locating events with a sparse network of regional arrays. Bull Seismol Soc Am 78(2):780–798

Bronk-Ramsey C (2009) Bayesian analysis of radiocarbon dates. Radiocarbon 51:337–360

Cecic I, Musson RM, Stucchi M (1996) Do seismologists agree upon epicentre determination from macroseismic data? A survey of ESC working group. Ann Geofis 39(5)

Daeron M, Klinger Y, Tapponnier P, Elias A, Jacques E, Sursock A (2005) Sources of the large 1202AD and 1759 near east earthquakes. Geology 33(7):529–532

Daeron M, Klinger Y, Tapponnier P, Elias A, Jacques E, Sursock A (2007) 12,000-year-long record of 10 to 13 paleoearthquakes

on the Yammouneh fault, Levant fault system, Lebanon. Bull Seismol Soc Am 97(3):749–771
Danciu L, Kale O, Akkar S (2016) The 2014 Earthquake Model of the Middle East: ground motion model and uncertainties. Bull Earthq Eng:1–37
Danciu L, Sesetyan K, Demircioglu M, Guelen L, Zare et al (2017) The 2014 earthquake model of the Middle East: seismogenic sources. Bull Earthq Eng:1–32
Darawcheh R, Sbeinati MR, Margottini C, Paolini S (2000) The 9 July 551 AD Beirut earthquake, eastern Mediterranean region. J Earth Eng 04:403
Di Giacomo D, Bondar I, Storchak DA, Engdahl ER, Bormann P, Harris J (2015) ISC-GEM: Global Instrumental Earthquake Catalogue (1900–2009), III. Re-computed MS and mb, proxy MW, final magnitude composition and completeness assessment. Phys Earth Planet Interiors 239:33–47
Dunbar P (2009) Global significant earthquake database, National Oceanic and Atmospheric Administration (NOAA). Boulder, CO, USA. https://doi.org/10.7289/V5TD9V7K
Elias A, Tapponnier P, Singh SC et al (2007) Active thrusting offshore Mount Lebanon: source of the tsunamigenic AD 551 Beirut-Tripoli earthquake. Geology 35(8):755–758
Ellenblum R, Marco S, Agnon A, Rockwell T, Boas A (1998) Crusader castle torn apart by earthquake at dawn, 20 May 1202. Geology 26:303–306
Ellenblum R, Marco S, Kool R, Davidovitch U, Porat R, Agnon A (2015) Archaeological record of earthquake ruptures in Tell Ateret, the Dead Sea Fault. Tectonics 34(10):2105–2117
Feldman L & Amrat AQ (2007) Data file of historical earthquakes, GII Israel and NRA Jordan (unpublished)
Ferry M, Meghraoui M, Karaki NA, Al-Taj M, Khalil L (2011) Episodic behavior of the Jordan Valley section of the Dead Sea fault inferred from a 14-ka-long integrated catalog of large earthquakes. Bull Seismol Soc Am 101(1):39–67
Field EH, Arrowsmith RJ, Biasi GP, Bird P et al (2014) Uniform California earthquake rupture forecast, version 3 (UCERF3)—the time-independent model. Bull Seismol Soc Am 104(3):1122–1180
Field EH, Biasi GP, Bird P, Dawson TE et al (2015) Long-term time-dependent probabilities for the third Uniform California Earthquake Rupture Forecast (UCERF3). Bull Seismol Soc Am 105(2A):511–543
Gardner JK, Knopoff L (1974) Is the sequence of earthquakes in Southern California, with aftershocks removed, Poissonian? Bull Seism Soc Am 64(5):1363–1367
Garfunkel Z (2009) The long-and short-term lateral slip and seismicity along the Dead Sea Transform: an interim evaluation. Isr J Earth Sci 58:217–235
Garfunkel Z, Zak I, Freund R (1981) Active faulting in the Dead Sea rift. Tectonophysics 80(1–4):1–26
Gasperini P (2004) Boxer, version 3.3, http://gaspy.df.unibo.it/paolo/boxer/boxer.html.
Gasperini P, Bernardini F, Valensise G, Boschi E (1999) Defining seismogenic sources from historical felt reports. Bull Seismol Soc Am 89:94–110
Gasperini P, Vannucci G, Tripone D, Boschi E (2010) The location and sizing of historical earthquakes using the attenuation of macroseismic intensity with distance. Bull Seismol Soc Am 100(5A):2035–2066
Gomez F, Meghraoui M, Darkal AN, Hijazi et al (2003) Holocene faulting and earthquake recurrence along the Serghaya branch of the Dead Sea fault system in Syria and Lebanon. Geophys J Int 153(3):658–674
Goodman-Tchernov BN, Dey HW, Reinhardt EG, McCoy F, Mart Y (2009) Tsunami waves generated by the Santorini eruption reached Eastern Mediterranean shores. Geology 37(10):943–946
Grigoratos I, Dabeek J, Faravelli M, Di Meo A, Cerchiello V, Borzi B, Monteiro R, Ceresa P (2016) Development of a fragility and exposure model for Palestine - application to the city of Nablus. Procedia Eng 161:2023–2029. https://doi.org/10.1016/j.proeng.2016.08.797
Grigoratos I, Monteiro R, Ceresa P, Di Meo A, Faravelli M, Borzi B (2018a) Crowdsourcing exposure data for seismic vulnerability assessment in developing countries. J Earthq Eng:1–18. https://doi.org/10.1080/13632469.2018.1537901
Grigoratos I, Danciu L, Poggi V, Rojo G, Monteiro R & Ceresa P (2018b) Data harmonization and earthquake-rate forecast for the Palestinian territories. 11th United States National Conference on earthquake engineering, Los Angeles, USA
Grigoratos I, Poggi V, Danciu L, Monteiro R (2020) Data-driven methods for merging and homogenizing instrumental earthquake catalogs – application to the Dead Sea Transform fault zone. Geophys J Int (under review)
Gruenthal G (1998) European macroseismic scale 1998 (EMS 1998). Council of Europe, Publication of the European Centre for Geodynamics and Seismology, 15
Gruenthal G, Wahlstroem R (2012) The European-Mediterranean Earthquake Catalogue (EMEC) for the last millennium. J Seismol 16(3):535–570
Guidoboni E & Comastri A (2005) Catalogue of earthquakes and tsunamis in the Mediterranean area from the 11th to the 15th century, Istituto nazionale di geofisica e vulcanologia
Guidoboni E, Comastri A & Traina G (1994) Catalogue of ancient earthquakes in the Mediterranean area up to the 10th century, Istituto Nazionale di Geofisica
Guidoboni E, Bernardini F, Comastri A, Boschi E (2004) The large earthquake on 29 June 1170 (Syria, Lebanon, and central southern Turkey). J Geophys Res 109(B07)
Guidoboni E, Ferrari G, Tarabusi G, Sgattoni G, Comastri A, Mariotti D et al (2019) CFTI5Med, the new release of the catalogue of strong earthquakes in Italy and in the Mediterranean area. Scie Data 6(1):80
Hanks TC, Kanamori H (1979) A moment magnitude scale. J Geophys Res 84(5):2348–2350
Haynes JM, Niemi TM, Atallah M (2006) Evidence for ground-rupturing earthquakes on the Northern Wadi Araba fault at the archaeological site of Qasr Tilah, Dead Sea Transform fault system, Jordan. J Seismol 10(4):415–430
Hiemer S, Woessner J, Basili R, Danciu L, Giardini D, Wiemer S (2014) A smoothed stochastic earthquake rate model considering seismicity and fault moment release for Europe. Geophys J Int 198(2):1159–1172
Hough SE, Avni R (2009) The 1170 and 1202 CE Dead Sea Rift earthquakes and long-term magnitude distribution of the Dead Sea fault zone. Isr J Earth Sci 58:295–308
Kagan E, Stein M, Agnon A, Neumann F (2011) Intrabasin paleoearthquake and quiescence correlation of the late Holocene Dead Sea. J Geophys Res Solid Earth 116(B4)
Karcz I (2004) Implications of some early Jewish sources for estimates of earthquake hazard in the Holy Land. Ann Geophys 47(2–3)

Ken-Tor R, Agnon A, Enzel Y, Stein M, Marco S, Negendank JF (2001a) High-resolution geological record of historic earthquakes in the Dead Sea basin. J Geophys Res Solid Earth 106(B2):2221–2234

Ken-Tor R, Stein M, Enzel Y, Agnon A, Marco S, Negendank JF (2001b) Precision of calibrated radiocarbon ages of historic earthquakes in the Dead Sea basin. Radiocarbon 43(03): 1371–1382

Khair K, Karakaisis GF & Papadimitriou EE (2000) Seismic zonation of the Dead Sea transform fault area. Ann Geofys 43(1)

Klinger Y, Avouac JP, Dorbath L, Abou-Karaki N, Tisnerat N (2000) Seismic behaviour of the Dead Sea fault along Araba Valley, Jordan. Geophys J Int 142:769–782

Klinger Y, Le Beon M, Al-Qaryouti M (2015) 5000 yr of paleoseismicity along the southern Dead Sea fault. Geophys J Int 202(1):313–327

Kottmeier C, Agnon A, Al-Halbouni D, Alpert P, Corsmeier U, Dahm T et al (2016) New perspectives on interdisciplinary earth science at the Dead Sea: the DESERVE project. Sci Total Environ 544:1045–1058

Langgut D, Yannai E, Taxel I, Agnon A, Marco S (2016) Resolving a historical earthquake date at Tel Yavneh (central Israel) using pollen seasonality. Palynology 40(2):145–159

López-Merino L, Leroy SA, Eshel A, Epshtein V, Belmaker R, Bookman R (2016) Using palynology to re-assess the Dead Sea laminated sediments–indeed varves? Quat Sci Rev 140: 49–66

Lowe DR (1975) Water escape structures in coarse grained sediments. Sedimentology 22

Marco S, Klinger Y (2014) Review of on-fault palaeoseismic studies along the Dead Sea fault. In: Garfunkel Z, Ben-Avraham Z, Kagan E (eds) Dead Sea Transform Fault System: Reviews. Springer

Marco S, Stein M, Agnon A, Ron H (1996) Long-term earthquake clustering: a 50,000-year paleoseismic record in the Dead Sea Graben. J Geophys Res: Solid Earth 101(B3):6179–6191

Marco S, Agnon A, Ellenblum R, Eidelman A, Basson U, Boas A (1997) 817-year-old walls offset sinistrally 2.1m by the Dead Sea Transform. Israel J Geodyn 24:11–20

Marco S, Hartal M, Hazan N, Lev L, Stein M (2003) Archaeology, history, and geology of the A.D. 749 earthquake, dead sea transform. Geology 31(8):665–668

Marco S, Rockwell TK, Heimann A, Frieslander U, Agnon A (2005) Late Holocene activity of the Dead Sea Transform revealed in 3D palaeoseismic trenches on the Jordan Gorge segment. Earth Planet Sci Lett 234(1):189–205

Masson F, Hamiel Y, Agnon A, Klinger Y, Deprez A (2015) Variable behavior of the Dead Sea fault along the southern Arava segment from GPS measurements. Compt Rendus Geosci 347(4):161–169

Meghraoui M, Gomez F, Sbeinati R, Van der Woerd J, Mouty M, Darkal AN, Radwan Y, Layyous I, Al Najjar H, Darawcheh R, Hijazi F, Al-Ghazzi R, Barazangi M (2003) Evidence for 830 years of seismic quiescence from palaeoseismology, archaeoseismology and historical seismicity along the Dead Sea fault in Syria. Earth Planet Sci Lett 210(1):35–52

Mignan A, Danciu L, Giardini D (2015) Reassessment of the maximum fault rupture length of strike-slip earthquakes and inference on M_{max} in the Anatolian Peninsula, Turkey. Seismol Res Lett 86(3):890–900

Migowski C, Agnon A, Bookman R, Negendank JF, Stein M (2004) Recurrence pattern of Holocene earthquakes along the Dead Sea transform revealed by varve-counting and radiocarbon dating of lacustrine sediments. Earth Planet Sci Lett 222(1):301–314

Molin D (1995) Considerations on the assessment of macroseismic intensity. Ann Geofis 38:5–6

Nemer T, Meghraoui M (2006) Evidence of coseismic ruptures along the Roum fault (Lebanon): a possible source for the AD 1837 earthquake. J Struct Geol 28(8):1483–1495

Nemer T, Meghraoui M, Khair K (2008) The Rachaya-Serghaya fault system (Lebanon): evidence of coseismic ruptures, and the AD 1759 earthquake sequence. J Geophys Res Solid Earth 113(B5)

Panzera F, Lombardo G, Rigano R (2011) Use of different approaches to estimate seismic hazard: the study cases of Catania and Siracusa, Italy. Boll Geofis Teor Appl 52(4)

Panzera F, Zechar JD, Vogfjörd KS, Eberhard DA (2016) A revised earthquake catalogue for South Iceland. Pure Appl Geophys 173(1):97–116

Pasolini C, Gasperini P, Albarello D, Lolli B, D'Amico V (2008) The attenuation of seismic intensity in Italy, part I: theoretical and empirical backgrounds. Bull Seismol Soc Am 98(2): 682–691

Plassard J and Kogoj B (1981) Seismicite du Liban: catalogue des seismes ressentis. Collection des Annales-Mémoires de l'Observatoire de Ksara, 3rd edition, vol. 4

Poirier JP, Taher MA (1980) Historical seismicity in the near and Middle East, North Africa, and Spain from Arabic documents (VIIth-XVIIIth century). Bull Seismol Soc Am 70(6):2185–2201

Reches ZE, Hoexter DF (1981) Holocene seismic and tectonic activity in the Dead Sea area. Tectonophysics 80(1):235–254

Rovida AN, Locati M, Camassi RD, Lolli B and Gasperini P (2016) CPTI15, the 2015 version of the Parametric Catalog of Italian Earthquakes. https://emidius.mi.ingv.it/CPTI15-DBMI15/description_CPTI15.htm

Rucker JD & Niemi TM (2010) Historical earthquake catalogues and archaeological data: achieving synthesis without circular reasoning. In: Sintubin M, Stewart, IS, Niemi, T M, Altunel E (eds) Ancient earthquakes Geol. soc.Am. special paper. pp 97–106

Russell KW (1985) The earthquake chronology of Palestine and Northwest Arabia from the 2nd through the mid-8th century AD. BASOR 260:37–59

Salamon A (2010) Patterns of seismic sequences in the Levant—interpretation of historical seismicity. J Seismol 14(2):339–367

Salamon A, Rockwell T, Ward SN, Guidoboni E, Comastri A (2007) Tsunami hazard evaluation of the eastern Mediterranean: historical analysis and selected modeling. Bull Seismol Soc Am 97(3):705–724

Sbeinati, M.R., Darawcheh, R. & Mouty, M., 2005. The historical earthquakes of Syria: an analysis of large seismic events from 1365 B.C. to 1900 A.D., Ann Geofis, 48,347–435

Shebalin NV (1970) Intensity: on the statistical definition of the term. In Proc. X Ass. ESC, Leningrad, Acad. Sci. USSR, Soviet Geophysical Committee, Moscow

Sibol MS, Bollinger GA, Birch JB (1987) Estimation of magnitudes in central and eastern North America using intensity and felt area. Bull Seismol Soc Am 77(5):1635–1654

Sieberg A (1932) Untersuchungen ueber Erdbeben und Bruchschollenbau im oestlichen Mittelmeersgebiet. Denkschr Mediz- Naturwiss Gesell Jena 2:184–224

Sun R, Vaccari F, Marrara F, Panza GF (1998) The main features of the local geological conditions can explain the macroseismic intensity caused in Xiji-Langfu (Beijing) by the M_S = 7.7 Tangshan 1976 Earthquake. Pure Appl Geophys 152(3):507–521

Thomas R, Parker ST, Niemi TM (2007) Structural damage from earthquakes in the second: ninth centuries at the archaeological site of Aila in Aqaba, Jordan. Bull Am Sch Orient Res:59–77

Wechsler N, Rockwell TK, Klinger Y, Stepancikova P, Kanari M, Marco S, Agnon A (2014) A paleoseismic record of earthquakes for the Dead Sea transform fault between the first and seventh centuries CE: nonperiodic behavior of a plate boundary fault. Bull Seismol Soc Am 104(3):1329–1347

Wells DL, Coppersmith KJ (1994) New empirical relationships among magnitude, rupture length, rupture width, rupture area, and surface displacement. Bull Seismol Soc Am 84(4):974–1002

Williams JB, Schwab MJ, Brauer A (2012) An early first-century earthquake in the Dead Sea. Int Geol Rev 54(10):1219–1228

Willis B (1928) Earthquakes in the Holy Land. Bull Seismol Soc Am 18:73–103

Woessner J, Laurentiu D, Giardini D, Crowley H, Cotton F, Grünthal G et al (2015) The 2013 European seismic hazard model: key components and results. Bull Earthq Eng 13(12): 3553–3596

Wood HO, Neumann F (1931) Modified Mercalli intensity scale of 1931. Bull Seismol Soc Am 21(4):277–283

Zare M, Amini H, Yazdi P, Sesetyan K, Demircioglu MB, Kalafat D et al (2014) Recent developments of the Middle East catalog. J Seismol 18(4):749–772

Zilberman E, Amit R, Porat N, Enzel Y, Avner U (2005) Surface ruptures induced by the devastating 1068 AD earthquake in the southern Arava valley, Dead Sea Rift, Israel. Tectonophysics 408(1):79–99

Zohar M, Salamon A, Rubin R (2016) Reappraised list of historical earthquakes that affected Israel and its close surroundings. J Seismol 20(30):971–985

Zohar M, Salamon A and Rubin R (2017) Earthquake damage history in Israel and its close surrounding - evaluation of spatial and temporal patterns: Tectonophysics

Zuhair H, McKnight S, Eaton D (2015) Historical seismicity of the Jordan Dead Sea Transform region and seismotectonic implications. Arab J Geosci 8(6):4039–4055